Introduction to Nanotechnology and Nanoscience – Class#12

Liwei Lin

Professor, Dept. of Mechanical Engineering
Co-Director, Berkeley Sensor and Actuator Center
The University of California, Berkeley, CA94720
e-mail: lwlin@me.berkeley.edu
http://www.me.berkeley.edu/~lwlin

Outline

- □ Review
- □ HW#4
- □ Paper 4
- □ CNT Applications – Supercapacitors

HW #4

University of California at Berkeley
College of Engineering
Mechanical Engineering Department

ME118/218N, Spring 2024 **Liwei Lin**

Problem Set #4

Due February 29 (Thursday)

Problem 1 (CNT Properties)

Visit and critically review the carbon nanotube information from the websites listed in the course homepage or other places

Briefly answer the following questions with no more than one sentence each.

a. About how many times stronger than steel is a carbon nanotube?
b. Can a nanotube be metallic or semiconducting? How and why?
c. Carbon nanotubes exhibit a number of different quantum effects. Briefly describe one observed phenomenon.
d. About how many times better than copper is a carbon nanotube in terms of thermal conductivity in theory?

HW #4

Problem 2 (CNT Properties)

For a (7, 3) single wall carbon nanotube (SWCNT) that you have worked on in HW#2, Calculate:

a. Diameter of CNT *d*
b. Chiral angle θ;
c. 1D unit cell length *T* (along the CNT axis);
d. Number of carbon atoms per unit cell *N*.

Draw on a paper with graphene model:

e. Cartesian axes x and y;
f. Unit vectors a_1 and a_2;
g. Chiral vector C_h;
h. Chiral angle θ;

HW#4, Problem 2

Carbon, Vol. 33, No. 7, pp. 883-891, 1995

0008-6223/95 $9.50 + .00

0008-6223(95)00017-8

PHYSICS OF CARBON NANOTUBES

M. S. DRESSELHAUS,[1] G. DRESSELHAUS,[2] and R. SAITO[3]

Graphene to CNT

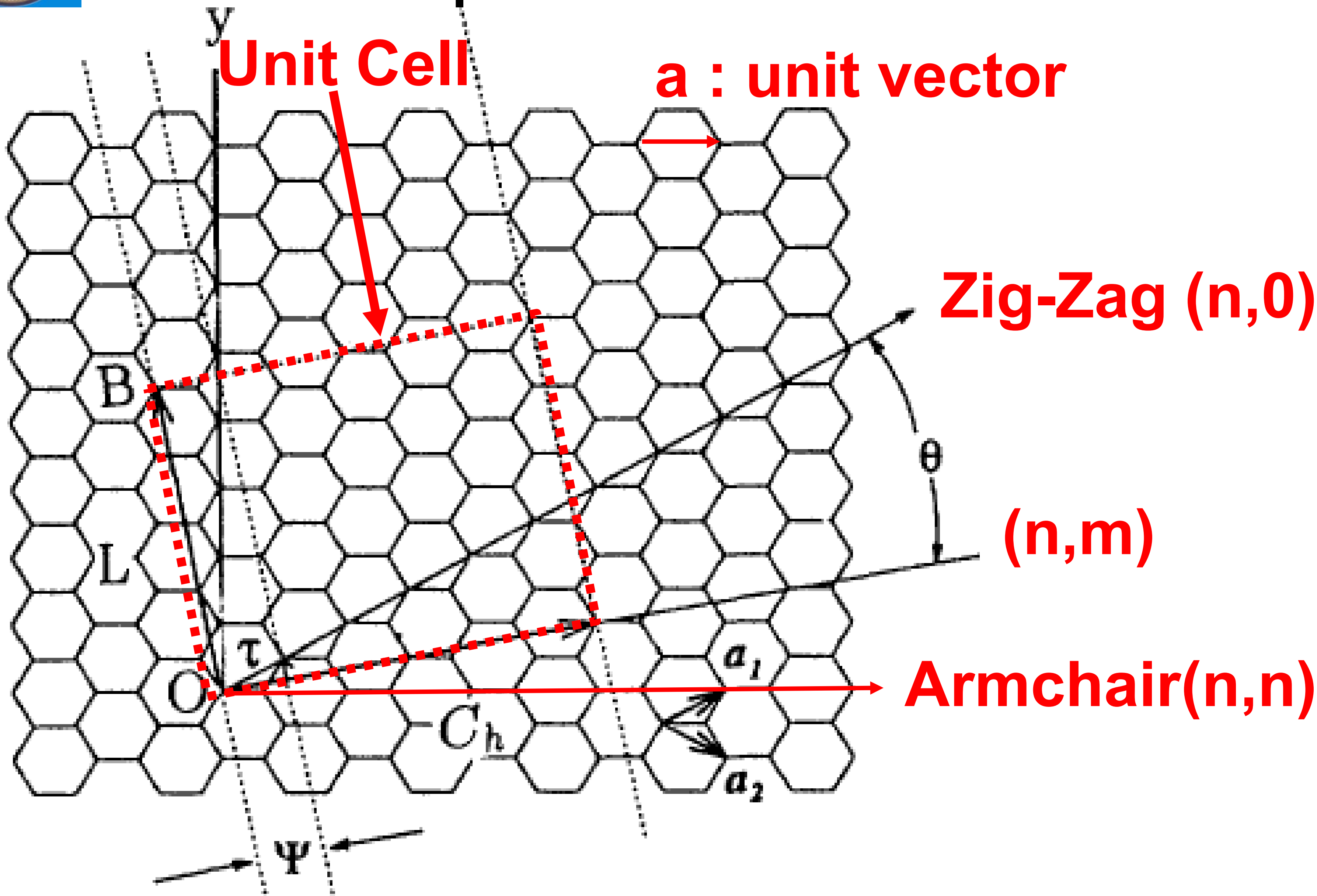

Chiral Vector

$$\mathbf{c}_h = n\mathbf{a}_1 + m\mathbf{a}_2, \qquad (1)$$

where $\mathbf{a}_1$ and $\mathbf{a}_2$ are the unit cell basis vectors of the 2D graphene sheet. By rolling the sheet so that this lattice point also coincides with the origin, a tubule specified by (n, m) is obtained. A chiral angle θ can be defined to be that between the zigzag direction and the vector $\mathbf{c}_h$; a zigzag tubule corresponds to $\theta = 0$ while for an armchair tubule the chiral angle is $\theta = \pi/6$. The smallest diameter zigzag and armchair tubules are believed to have a tubule circumference of $9a$ and $5\sqrt{3}a$, respectively, where a=2.46 Å is the in-plane lattice constant for graphite.

CNT Structure

We now define a unit cell along the tubule axis. Zigzag and armchair tubules can be considered as one-dimensional crystals with lattice constants of $\sqrt{3}a$ and a, respectively. To determine the lattice constant L of a chiral tubule as a function of n and m, we draw a straight line through O, in Fig. 1, normal to $\mathbf{c}_h$; the smallest lattice vector along this line has a length equal to that of $\overrightarrow{OB}$, where B is the first lattice point of the 2D graphene sheet through which this line passes. Since the lattice constant is the same for tubules specified by (n, m) or (ln, lm) for any integer l, it is sufficient to consider only those integers n and m which have no common divisor in describing the lattice constant L for a chiral tubule.

If $\hat{y}$ is a unit vector along the y axis in Fig. 1, then the angle between vectors $\overrightarrow{OB}$ and $\hat{y}$ is $\pi/6 - \theta$, and we can write

$$\tan(\pi/6 - \theta) = (n - m)/\sqrt{3}(n + m)\,. \tag{2}$$

CNT Structure Equations

$\mathbf{a}_1, \mathbf{a}_2$	unit vectors	$\left(\frac{\sqrt{3}}{2}, \frac{1}{2}\right) a, \left(\frac{\sqrt{3}}{2}, -\frac{1}{2}\right) a$
$\mathbf{C}_h$	chiral vector	$\mathbf{C}_h = n\mathbf{a}_1 + m\mathbf{a}_2 \equiv (n, m)$
L	circumference of nanotube	$L = \lvert\mathbf{C}_h\rvert = a\sqrt{n^2 + m^2 + nm}$
d_t	diameter of nanotube	$d_t = \frac{L}{\pi} = \frac{\sqrt{n^2 + m^2 + nm}}{\pi} a$
θ	chiral angle	$\sin\theta = \frac{\sqrt{3}m}{2\sqrt{n^2 + m^2 + nm}}$
		$\cos\theta = \frac{2n + m}{2\sqrt{n^2 + m^2 + nm}}$
		$\tan\theta = \frac{\sqrt{3}m}{2n + m}$

1D Translation Vector

T, where **T** is the 1D translation vector of the nanotube. The vector **T** is normal to $\mathbf{C}_h$ and extends from the origin to the first lattice point **B** in the honeycomb lattice. It is convenient to express **T** in terms of the integers (t_1, t_2) given in Table 1, where it is seen that the length of **T** is $\sqrt{3}L/d_R$ and d_R is either equal to the highest common divisor of (n, m), denoted by d, or to $3d$, depending on whether $n - m = 3dr$, r being an integer, or not (see Table 1). The number of carbon atoms per unit cell n_c of the 1D tubule is $2N$, as given in Table 1, each hexagon (or unit cell) of the honeycomb lattice containing two carbon atoms.

1D Translation Vector Equations

d	the highest common divisor of (n, m)	
d_R	the highest common divisor of $(2n + m, 2m + n)$	$d_R = \begin{cases} d & \text{if } n - m \text{ not a multiple of } 3d \\ 3d & \text{if } n - m \text{ a multiple of } 3d. \end{cases}$
$\mathbf{T}$	translational vector of 1D unit cell	$\mathbf{T} = t_1\mathbf{a}_1 + t_2\mathbf{a}_2 \equiv (t_1, t_2)$ $t_1 = \frac{2m + n}{d_R}$ $t_2 = -\frac{2n + m}{d_R}$
T	length of $\mathbf{T}$	$T = \frac{\sqrt{3}L}{d_R}$
N	number of hexagons per 1D unit cell	$N = \frac{2(n^2 + m^2 + nm)}{d_R}$

Table 1. Parameters of carbon nanotubes

Symbol	Name	Formula	Value
$a_{\text{C-C}}$	carbon-carbon distance		1.421 Å (graphite)
a	length of unit vector	$\sqrt{3}a_{\text{C-C}}$	2.46 Å
$\mathbf{a}_1, \mathbf{a}_2$	unit vectors	$\left(\frac{\sqrt{3}}{2}, \frac{1}{2}\right)a, \left(\frac{\sqrt{3}}{2}, -\frac{1}{2}\right)a$	in (x, y) coordinates
$\mathbf{b}_1, \mathbf{b}_2$	reciprocal lattice vectors	$\left(\frac{1}{\sqrt{3}}, 1\right)\frac{2\pi}{a}, \left(\frac{1}{\sqrt{3}}, -1\right)\frac{2\pi}{a}$	in (x, y) coordinates
$\mathbf{C}_h$	chiral vector	$\mathbf{C}_h = n\mathbf{a}_1 + m\mathbf{a}_2 \equiv (n, m)$	n, m: integers
L	circumference of nanotube	$L = \lvert\mathbf{C}_h\rvert = a\sqrt{n^2 + m^2 + nm}$	$0 \le \lvert m\rvert \le n$
d_t	diameter of nanotube	$d_t = \frac{L}{\pi} = \frac{\sqrt{n^2 + m^2 + nm}}{\pi}a$	
θ	chiral angle	$\sin\theta = \frac{\sqrt{3}m}{2\sqrt{n^2 + m^2 + nm}}$ $\cos\theta = \frac{2n + m}{2\sqrt{n^2 + m^2 + nm}}$ $\tan\theta = \frac{\sqrt{3}m}{2n + m}$	$0 \le \lvert\theta\rvert \le 30°$
d	the highest common divisor of (n, m)		
d_R	the highest common divisor of $(2n + m, 2m + n)$	$d_R = \begin{cases} d & \text{if } n - m \text{ not a multiple of } 3d \\ 3d & \text{if } n - m \text{ a multiple of } 3d. \end{cases}$	

CNT Structure

Chiral vector for (n_1, n_2) CNT

$$\mathbf{C}_{\mathrm{CNT}} = n_1\mathbf{a}_1 + n_2\mathbf{a}_2 = (n_1, n_2)$$

Tube diameter

$$d_{\mathrm{CNT}} = \frac{|\mathbf{C}_{\mathrm{CNT}}|}{\pi} = a\sqrt{n_1^2 + n_2^2 + n_1 n_2}$$

CNT "translation" vector

$$\mathbf{T}_{\mathrm{CNT}} = t_1\mathbf{a}_1 + t_2\mathbf{a}_2 = (t_1, t_2)$$

$$t_1 = \frac{2n_2 + n_1}{d_{\mathrm{R}}} \qquad t_2 = -\frac{2n_1 + n_2}{d_{\mathrm{R}}}$$

$d_{\mathrm{R}} =$ Greatest common devisor of $(2n_1 + n_2, n_1 + 2n_2)$

Number of hexagons in **nanotube** unit cell:

$$N_{\mathrm{CNT}} = \frac{2(n_1^2 + n_2^2 + n_1 n_2)}{d_{\mathrm{R}}}$$

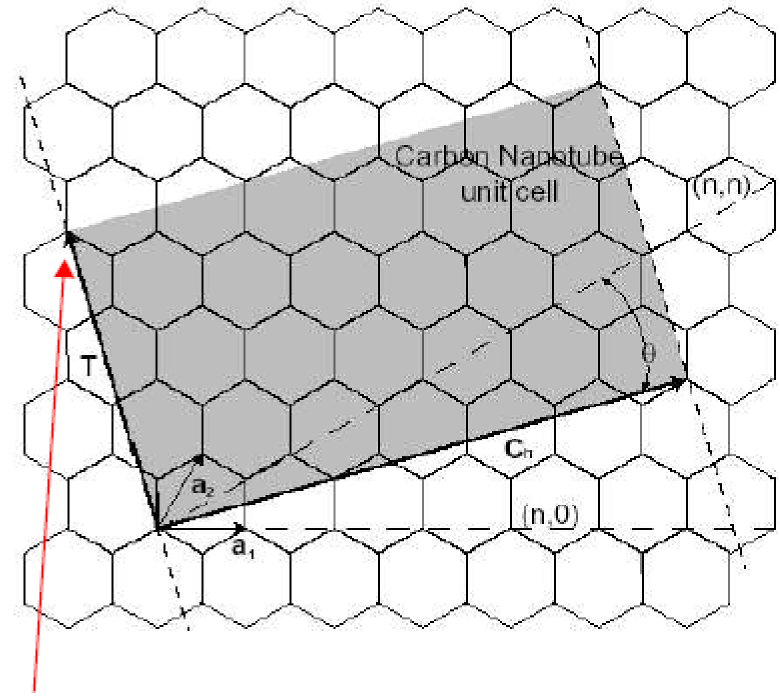

1st lattice point reached!

Chiral angle (definition)

$$\cos\theta = \frac{\mathbf{C}_{n_1,n_2} \cdot \mathbf{a}_1}{|\mathbf{C}_{n_1,n_2}||\mathbf{a}_1|} = \frac{2n_1 + n_2}{2\sqrt{n_1^2 + n_2^2 + n_1 n_2}}$$

CNT Composites’ Properties

- Conductivities of 0.01 to 0.1 S/cm for 5% loading
  - High electro conductivity can be achieved without subtracting from other material properties due to nanofiber morphology and low loading levels
- Unbundled SWNT’s reduce required loads as they enable lower percolation levels
  - Percolation thresholds as low as .1-.2% have been recorded in research
- Plastic semiconducting chip components prevent contaminants from carbon black sloughing

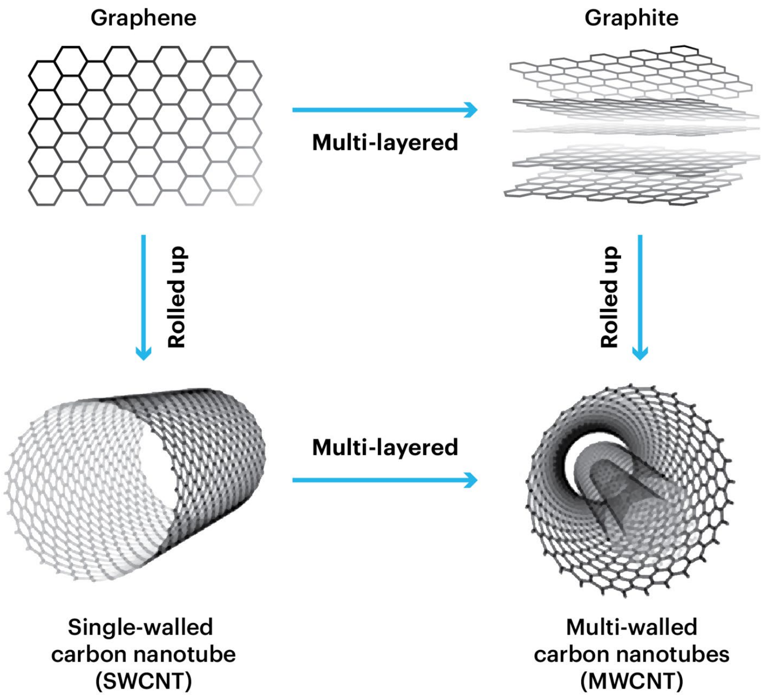

CNT Composites Properties Cont.

- Use of nanotubes within plastics can greatly increase modulus and strength
- Researchers have observed a monotonic increase to indentation by up to 350% on loading up to 2% of SWNT's
  - Have also observed a 200% of thermal conductivity with 1% of SWNT's
- 1% of loading in polystyrene increases the modulus by up to 42%
- 1% of loading in polystyrene increases the breaking stress by up to 25%

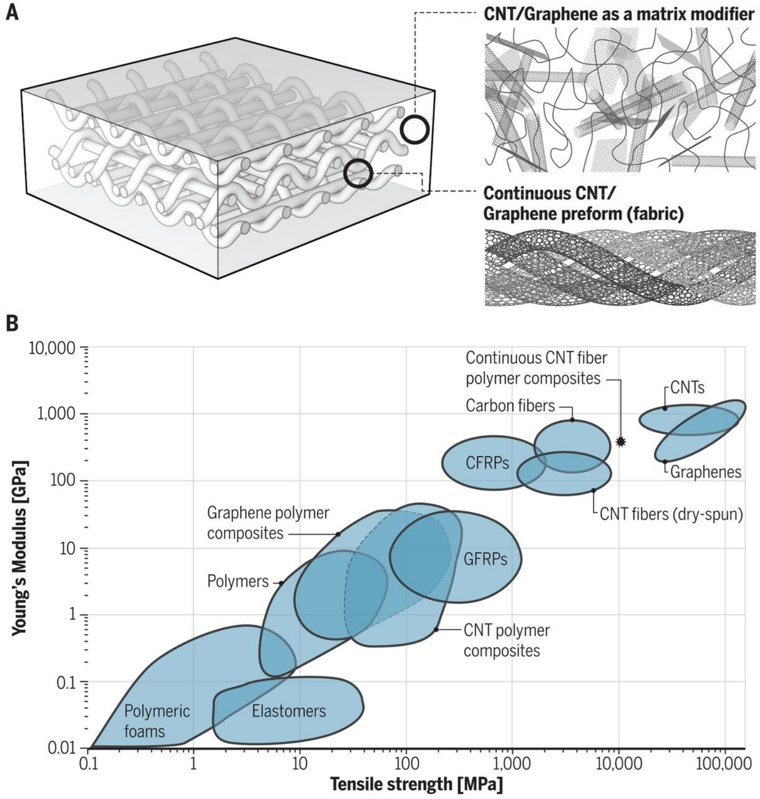

Applications of CNT Composites

- Can be used commercially in to prevent electric charge build up in gas lines and prevent explosions
- Better maintains barriers, stopping diffusion of fuel
- Used for plastic conductive automotive parts
- Incorporated in mirror housings that must be electrostatically painted
  - Smoothness of finish is better than other types of conductive fillers used
- Shielding from electromagnetic radiation from cellular devices and computers is possible using specially molded SWNT's and MWNT's

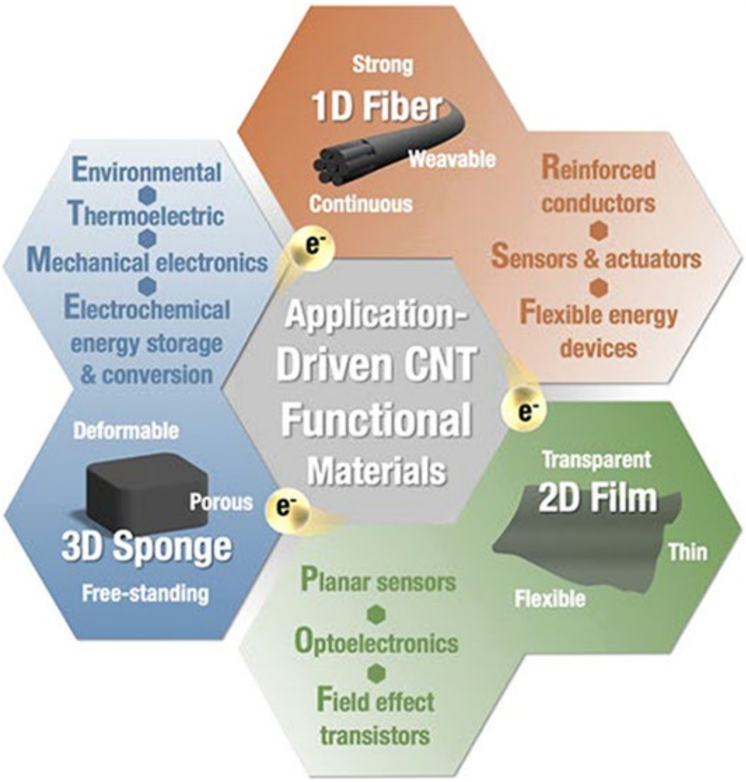

CNT Supercapacitor

- Capacitance depends on the separation between the charge on the electrolyte and the opposing charge in the electrolyte
- Distance between charges is typically ~1nm, unlike ~μm in dielectric capacitors
- Very high capacitances result from the large surface area of the nanotube
- A discharge time of ~7ms was found when 10 MWNT were connected in series at 10V
- The current largest reported reversible capacity is 1000 mA* hour/g for SWNT’s

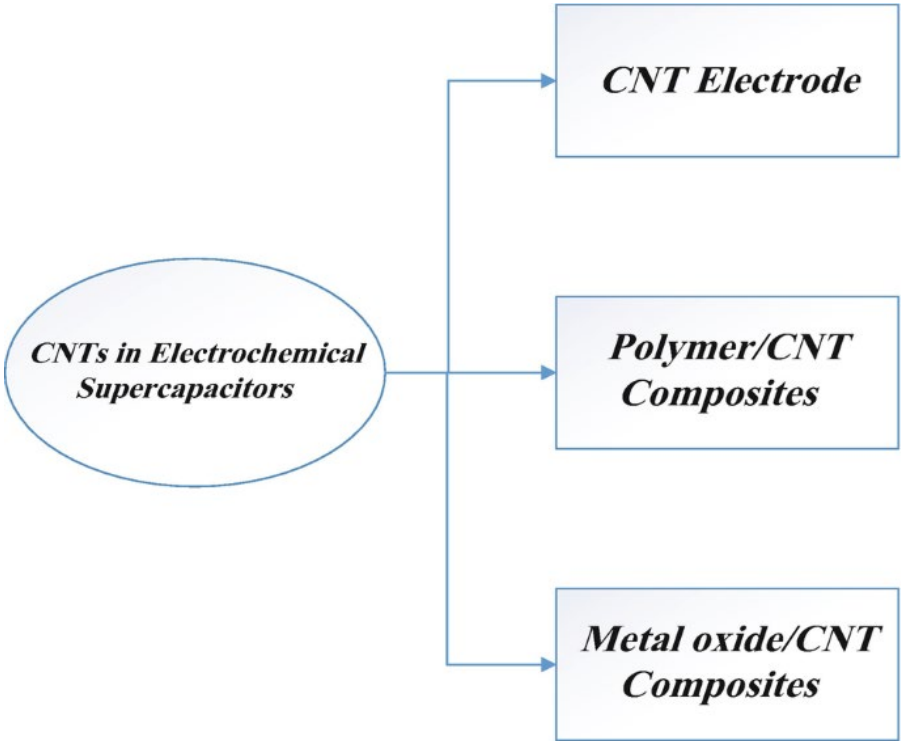

CNT Actuator

- Function at very low volts as compared to piezoelectric stack and electrostrictive actuators
- Have actuated at temperatures as high as 350° C and it is believed that up to 1000° C is feasible
- Maximum observed stress of SWNT actuator is 26 Mpa which is ~100x greater than muscle
    - But this is still ~100x lower than was predicted based off of the modulus of individual SWNT's
- The actuation of nanotubes depends on ion diffusion, so ferroelectrics can be cycled faster

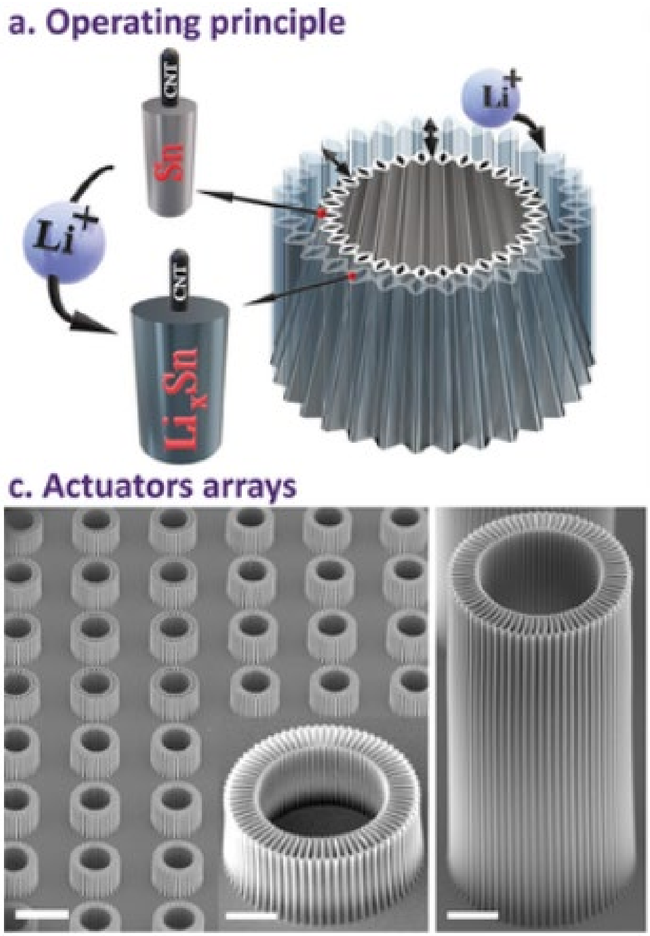

Sensors and Probes

Chemical Sensors:

- Possible with non-metallic tubes due to their electron transport and thermal sensitivity with applied charge.
- The advantage is their responsiveness at such a small size.
- The challenge is to provide both forward and reverse responses as well as differentiating substances in mixtures.

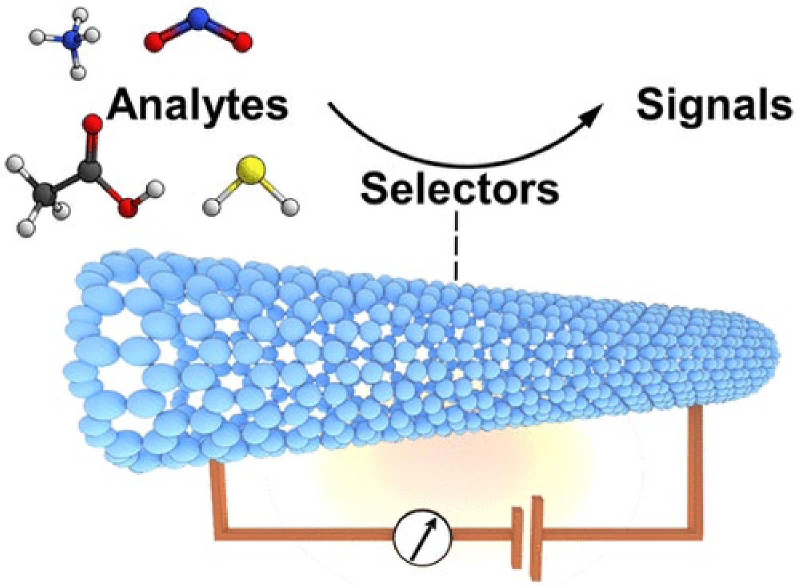

Sensors and Probes

Scanning Probe Tips for Atomic Microscopes:

- The durability and "low buckling force" extends probe life and better protects the sample upon contact.
- The cylindrical geometry and small diameter of the tube increases the imaging resolution compared to existing nanoprobes and allows for imaging in "narrow, deep crevices."
- Chemical and biological imaging is possible by "Covalently modifying" the probe tip.

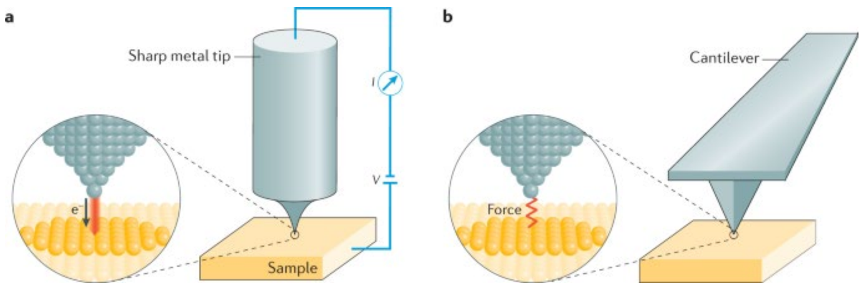

Sensors and Probes

Nanoscopic Tweezers:

- Actuated by “the electrostatic interaction betw two nanotubes.”
- Allows for manipulation of individual nanosctructures.
- Can probe for electrical properties of nanostructes.

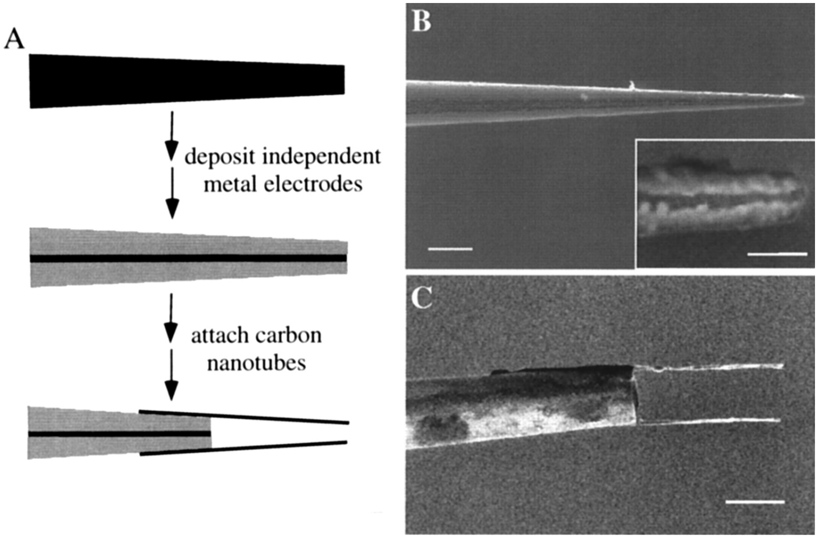

Sensors and Probes

Nanoscopic Tweezers:

- Applications include quantum dot and wire assemblies
- Possible future application of manipulating structures within cells.
- Figure shows manipulation of polystyrene nanoclusters

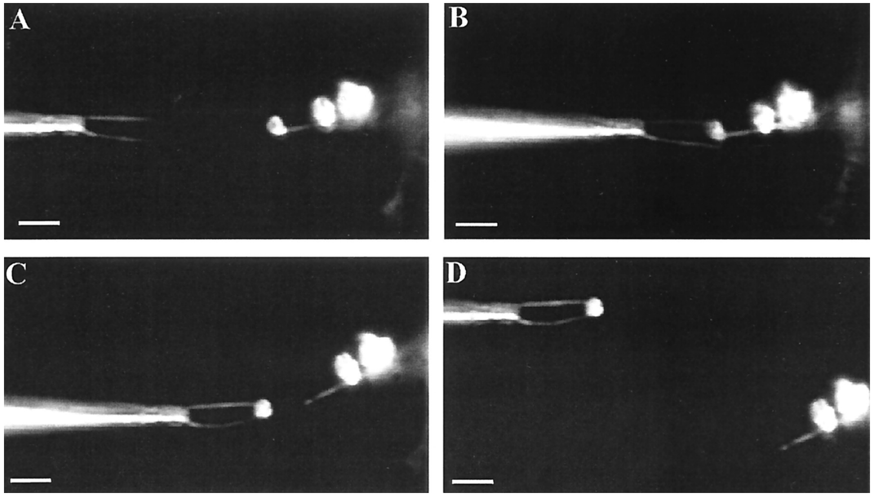

Sources

- J. C. Moses, et al. *Carbon Nanotubes and Their Polymer Nanocomposites: Raw Materials to Applications.* Elsevier, **2019**
- A Takakura, K. Beppu, T. Nishihara, A. Fukui , et all. “Strength of carbon nanotubes depends on their chemical structures” *Nature Communications, 3040, **2019.***
- B. Ribeiro, E. Botelho, M. Costa, C. Bandeira. “Carbon nanotube buckypaper reinforced polymer composites; a review” *Polimeros*, (**2017**)
- Baumans, X., Lombardo, J., Brisbois, J., Shaw, G., Zharinov, V., He, G., Yu, H., Yuan, J., Zhu, B., Jin, K., Kramer, R., Van De Vondel, J., & Silhanek, A. (2017).

  Healing effect of controlled anti-electromigration on conventional and high-T c superconducting nanowires. https://doi.org/10.1002/smll.201700384)
- Read, D. T., V.K. Tewary, & Gerstle, W. H. (2011). Modeling electromigration using the peridynamics approach. *Elsevier EBooks*, 45–69.

  https://doi.org/10.1533/9780857093752.1.45
- Lian-Mao Peng, Zhiyong Zhang, Sheng Wang (2014) Carbon nanotube electronics: recent advances. Materials Today. Volume 17, Issue 9. Pages 433-442. Recovered from: https://doi.org/10.1016/j.mattod.2014.07.008.
- Vera Schroeder, Suchol Savagatrup, Maggie He, Sibo Lin, and Timothy M. Swager, Chemical Reviews 2019 *119* (1), 599-663, DOI: 10.1021/acs.chemrev.8b00340
- Bian, K., Gerber, C., Heinrich, A.J. *et al.* Scanning probe microscopy. *Nat Rev Methods Primers* 1, 36 (2021). https://doi.org/10.1038/s43586-021-00033-2
- Philip Kim, Charles M. Lieber ,Nanotube Nanotweezers.*Science***286**,2148-2150(1999).DOI:10.1126/science.286.5447.2148

Electrochemical Energy Storage

High energy density ⟷ **High power density**

Fuel Cells | Batteries | Supercapacitors | Capacitors

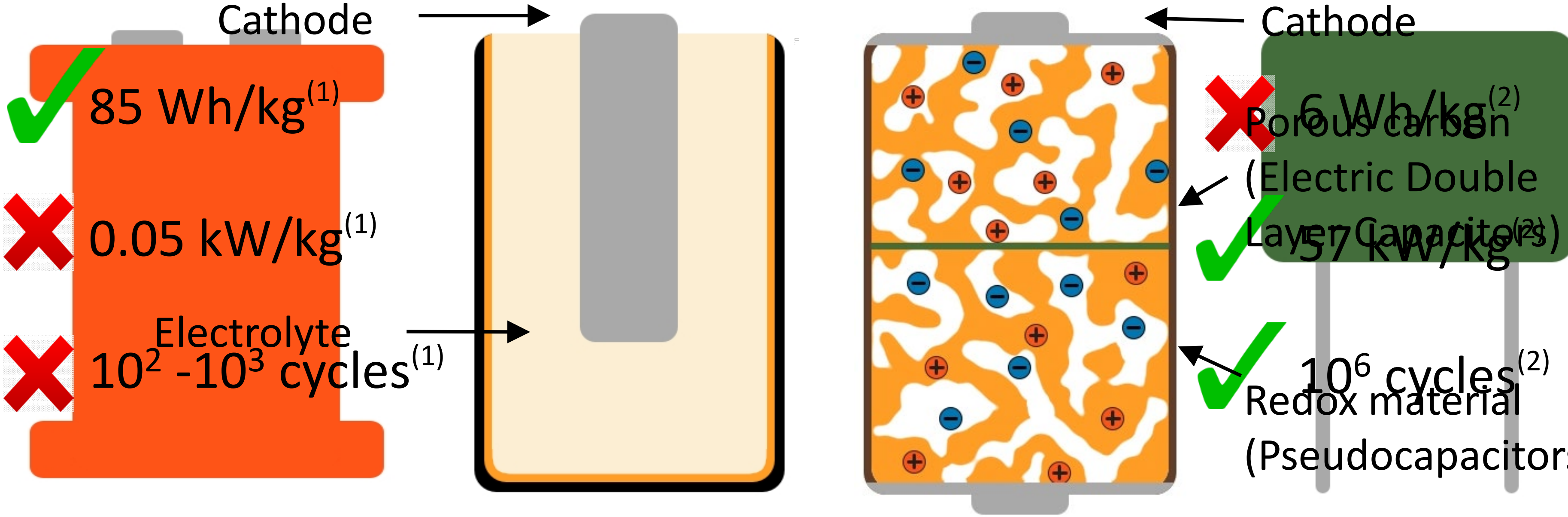

1) D. Linden, T. Reddy, *Handbook of Batteries*, McGraw-Hill, 2002.
http://www.eng.fiu.edu/mme/Robotics/elib/RehargeableBatteries-Paper-MEI-2012.pdf
2) Skeletontech, "SkelCap 2500, 4500, 3300, 4000" datasheet, December 2012.

State of the Field

Pseudocapacitors

Pseudocapacitive Material

RuO_2

MnO_2

Fe_3O_4

VO_x

Conductive polymers *

High Surface-Area Electrode

Activated carbon

Carbon nanotubes (CNTs)

Mesoporous carbon

Carbon aerogel

Energy Storage Overview

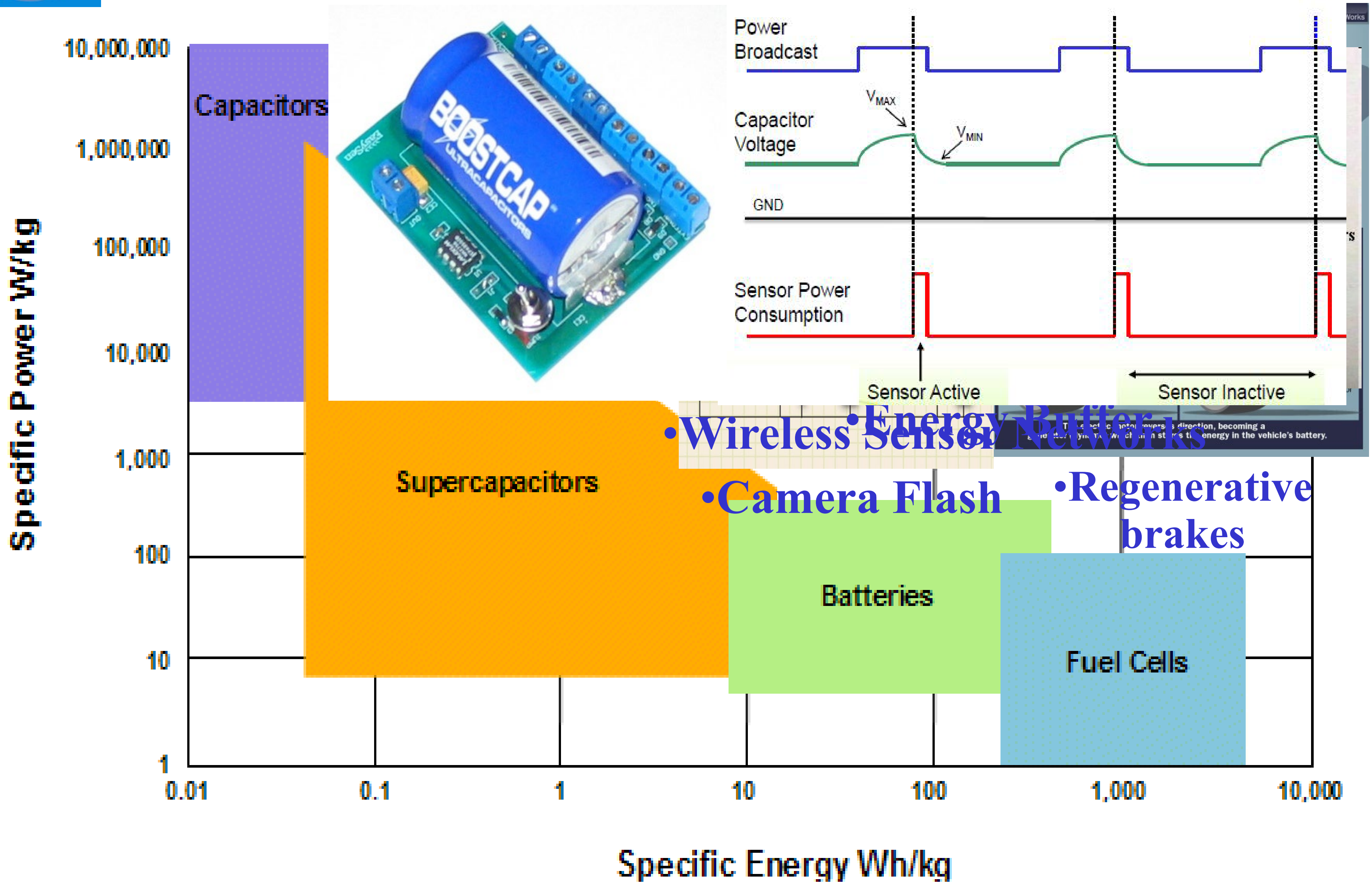

- •Energy Buffer
- •Wireless Sensor Networks
- •Camera Flash
- •Regenerative brakes

MEMS/Nano Battery

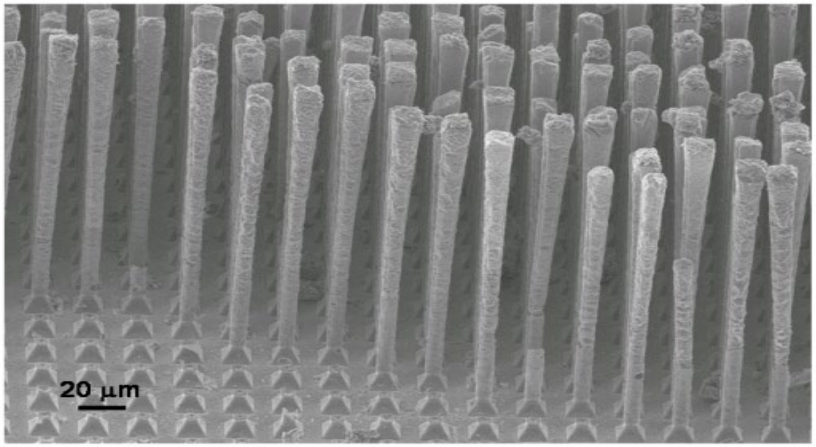

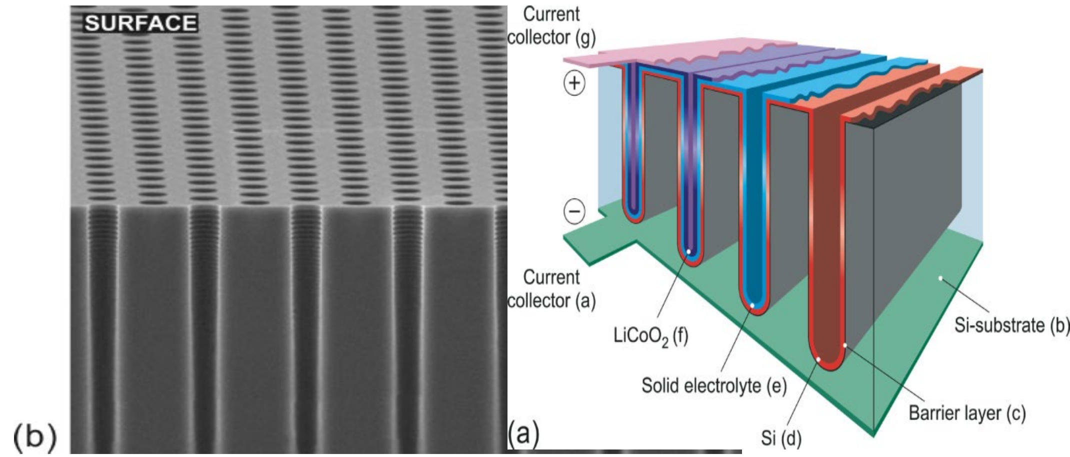

- ***Zinc-Air (UCLA) Electroplating, 10µm diameter, 200µm high***

- **Li-ion battery on Silicon, (Philips)** ***DRIE, 1µm gap, 25µm Deep***

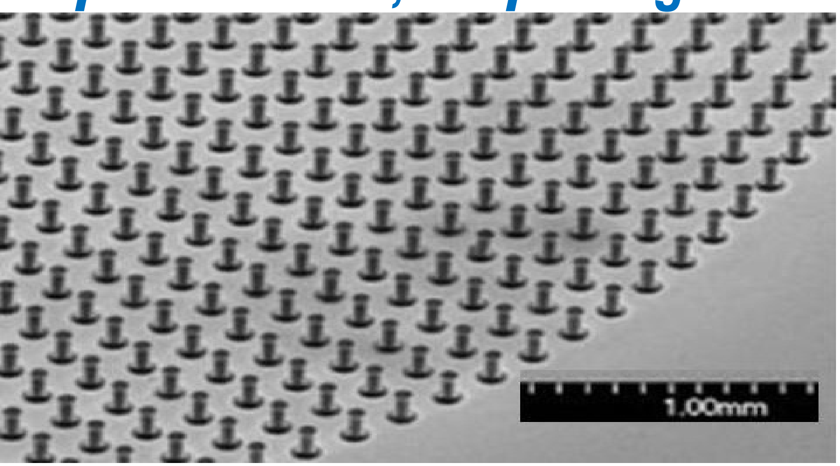

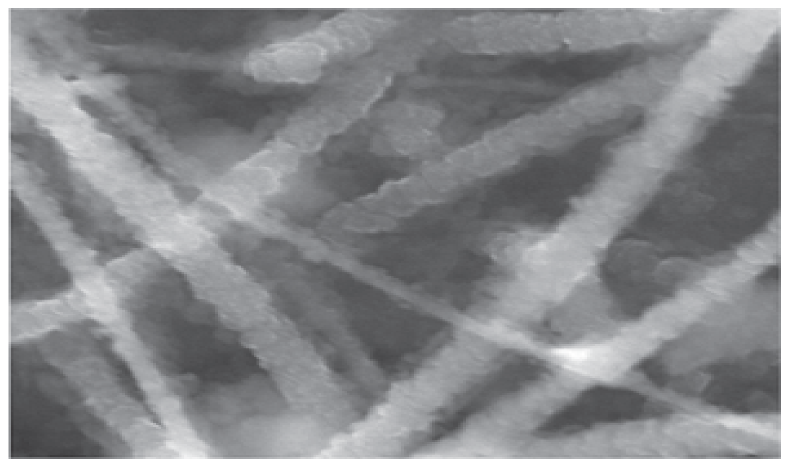

- **C-MEMS, (UCI),** ***SU8 pyrolysis 10µm diameter, 200µm high***

- **Si Nanowire, Li-ion battery, (Stanford),** ***~100nm diameter***

Supercapacitor

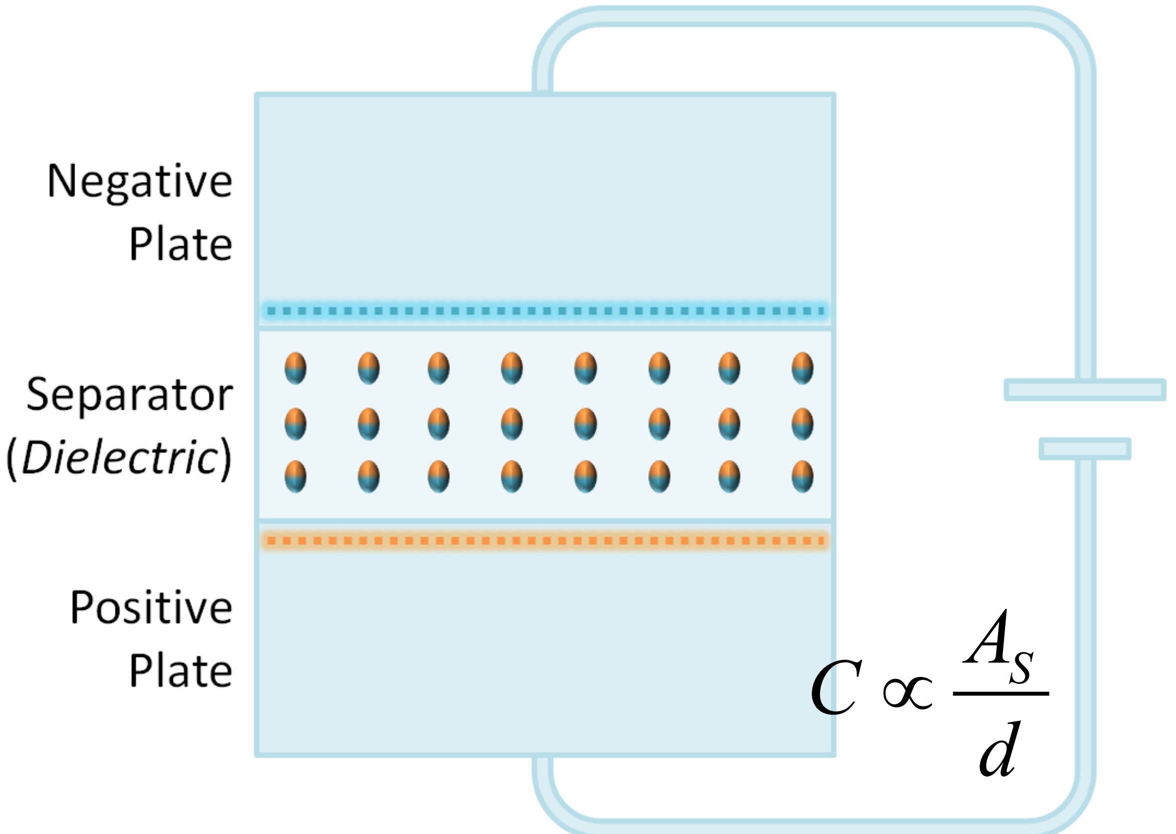

$$C \propto \frac{A_S}{d}$$

CNT-based Supercapacitor

- □Motivation
- □Micro Supercapacitor
  - Stage 1: CNT forest electrodes
  - Stage 2: Functionalized CNT electrodes
  - Stage 3: Ultra-long CNT electrodes
  - Stage 4: Deeply-packed CNT electrodes
- □Micro Battery
- □Summary

I. Carbon Nanotube Forest Electrodes

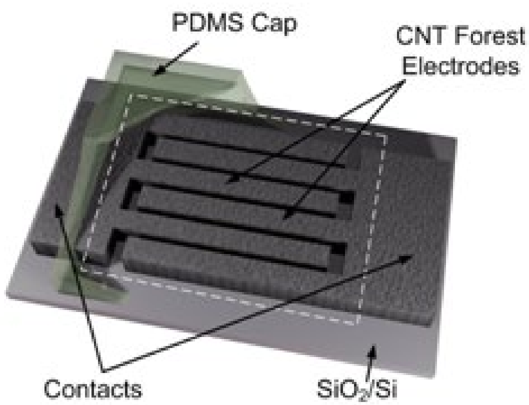

MEMS Supercapacitor

$$C_{SP} = \frac{C_I + C_E}{V} = \frac{\frac{\varepsilon}{d} A \uparrow + C_E}{V}$$

Aligned CNT Electrodes

	Activated Carbon [1]	Carbon Aerogel [2]	Carbon Nanotube
SEM	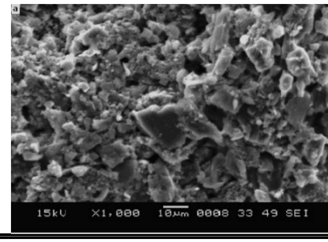	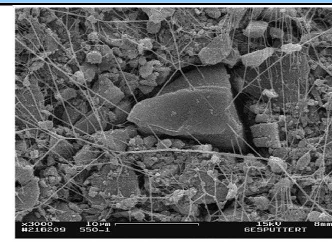	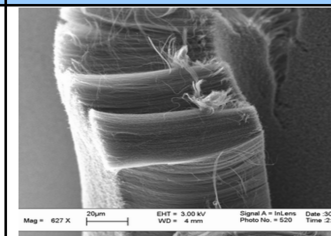
Pore Illustration	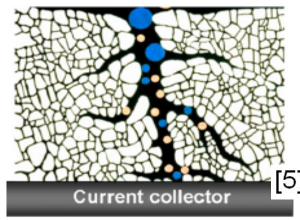	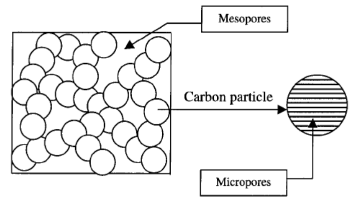	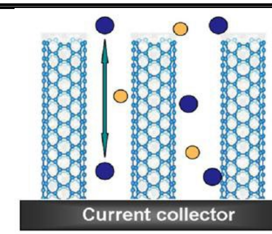
Specific capacitance @KOH (F/g)	27-80[6]	35[7]	90[3]
Conductivity (S/cm)	0.1[3]	2.5 [2]	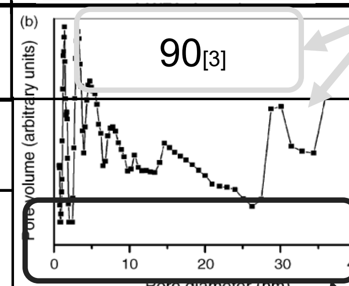
Contact Resistance	Powder-to-power Powder-to-sub	Powder-to-power Powder-to-sub	
Ion Diffusion Resistance	Power-like Network	Tablet-like Network	Vertical Network

Energy density

$$E = \frac{1}{2} C V_{\max}^2$$

$$C = \frac{\varepsilon_0 \varepsilon_r A_S}{d}$$

Power density

$$P_{\max} = \frac{V_{\max}^2}{4R_s}$$

CNT Growth on conductive substrates

Metal type	Ti (50)	Cr (50)	Ni (50)
Resistance before growth, R1	145	140	21
Resistance after growth, R2	11.7k	49.6k	373
Ratio of R2/R1	>80	>354	>17
CNT profile	Short and sparse	Long but sparse	Hardly any
SEM pictures	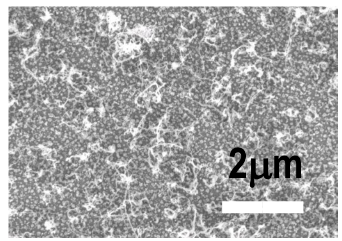	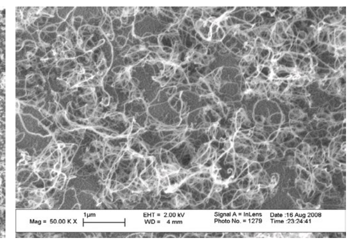	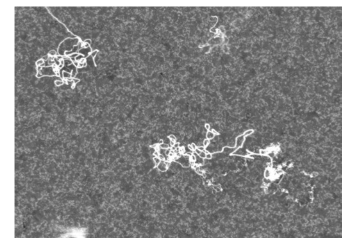
Metal type (cont.)	**Al (50)**	**Mo (50)**	**Mo/Al (50/10)**
Resistance before growth, R1	7.5	233	216
Resistance after growth, R2	16.7k	40	26
Ratio of R2/R1	>15560	~0.17	~0.12
CNT profile	Thick and dense	No at all	Thick and dense
SEM pictures	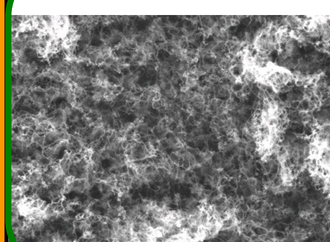	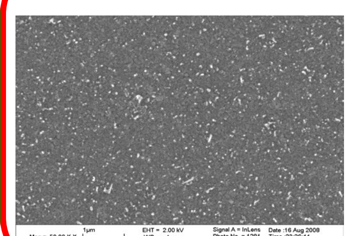	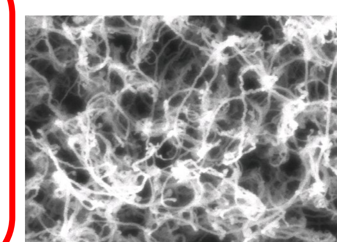

5nm Fe as the catalyst for all the samples

Fabrication process

1. Thermal oxidation
2. **Lithography**
3. ***Deposit metal layers***
4. **Lift-off**
5. ***CNT thermal CVD growth***
6. **Assembly**

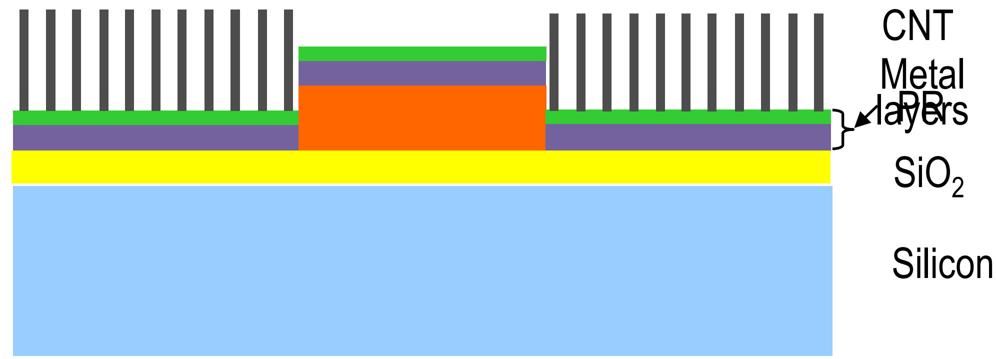

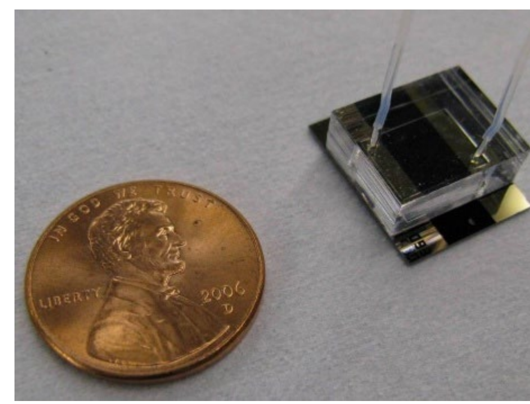

Supercapacitor electrodes using CNT Forests

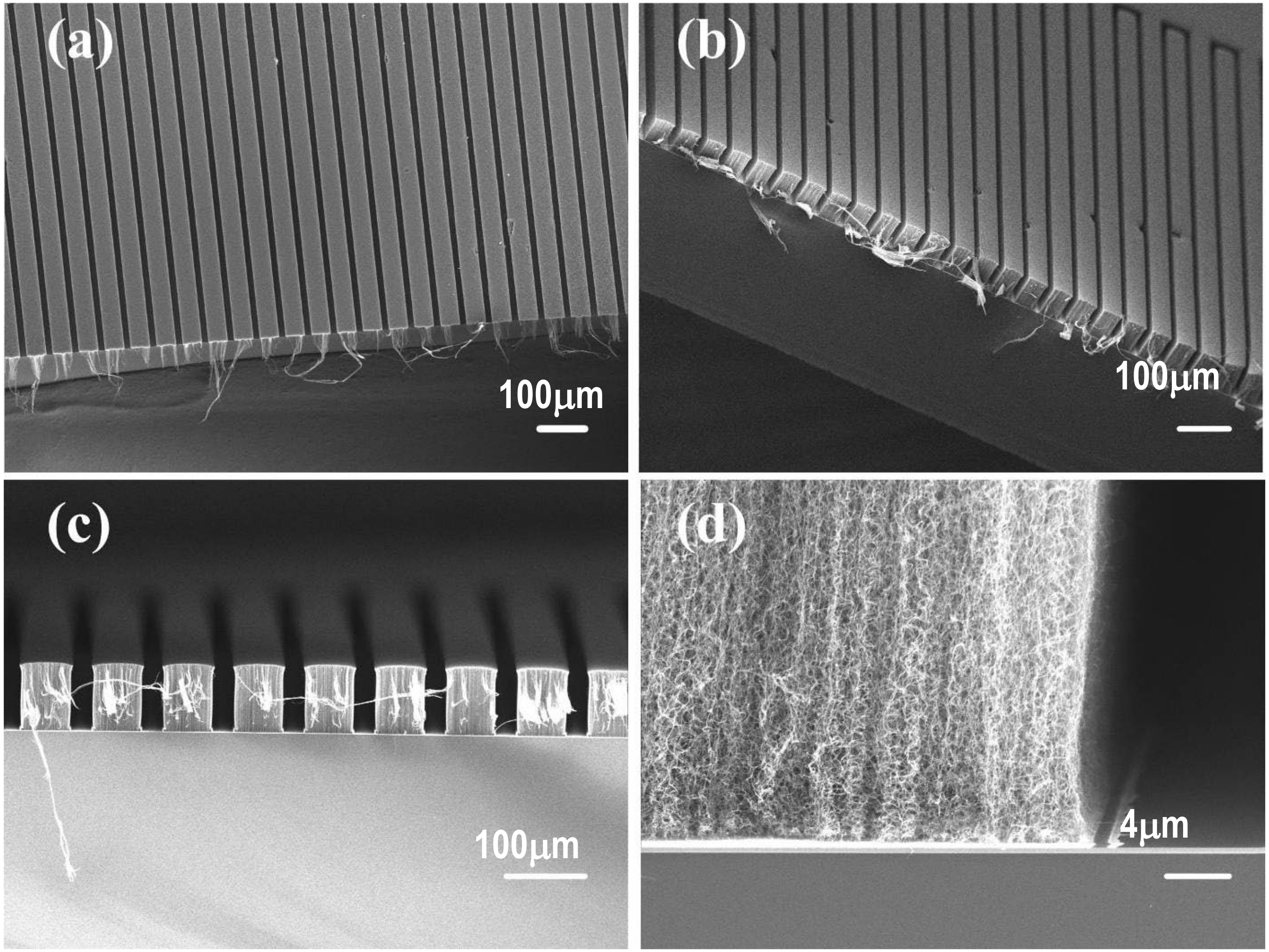

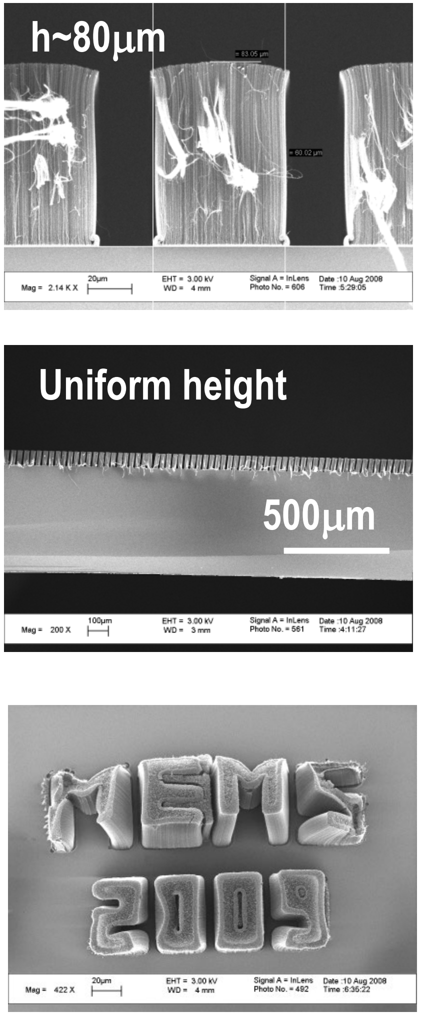

Performance of as-grown CNT supercapacitor

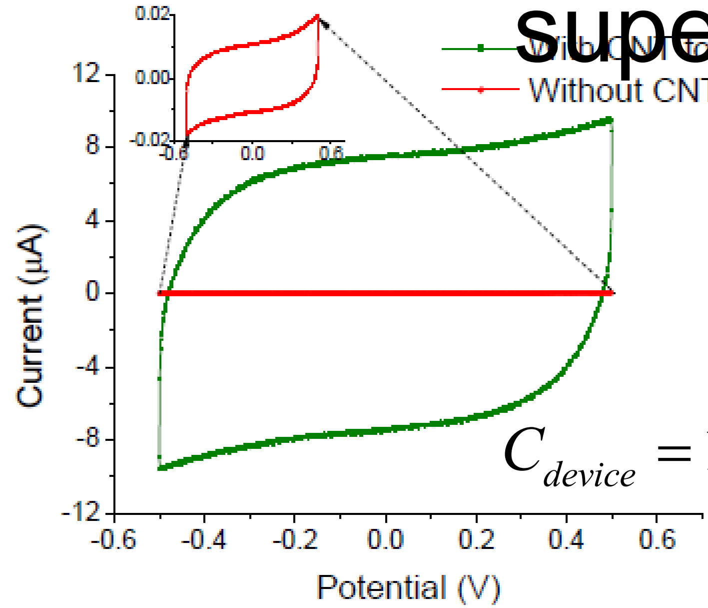

$$C_{device} = 150\mu F$$

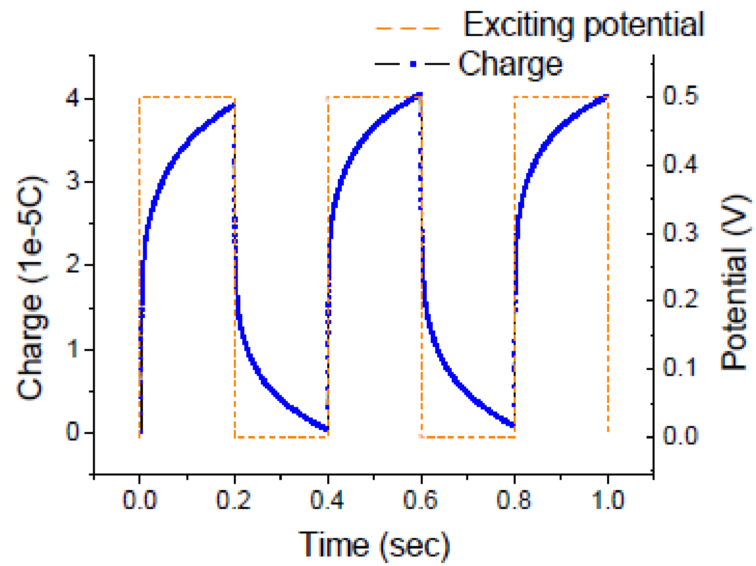

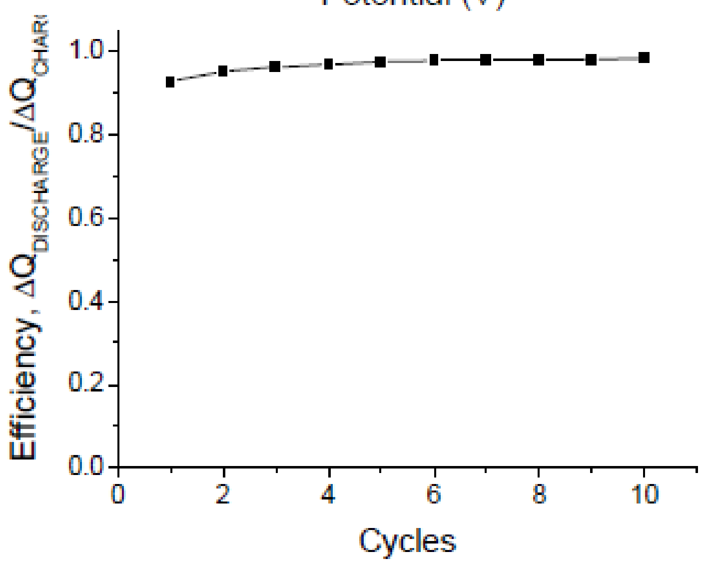

- 1000 times better in terms of capacitance
- High charge efficiency (>92%)
- Robust operation

Relative Location Among Peers

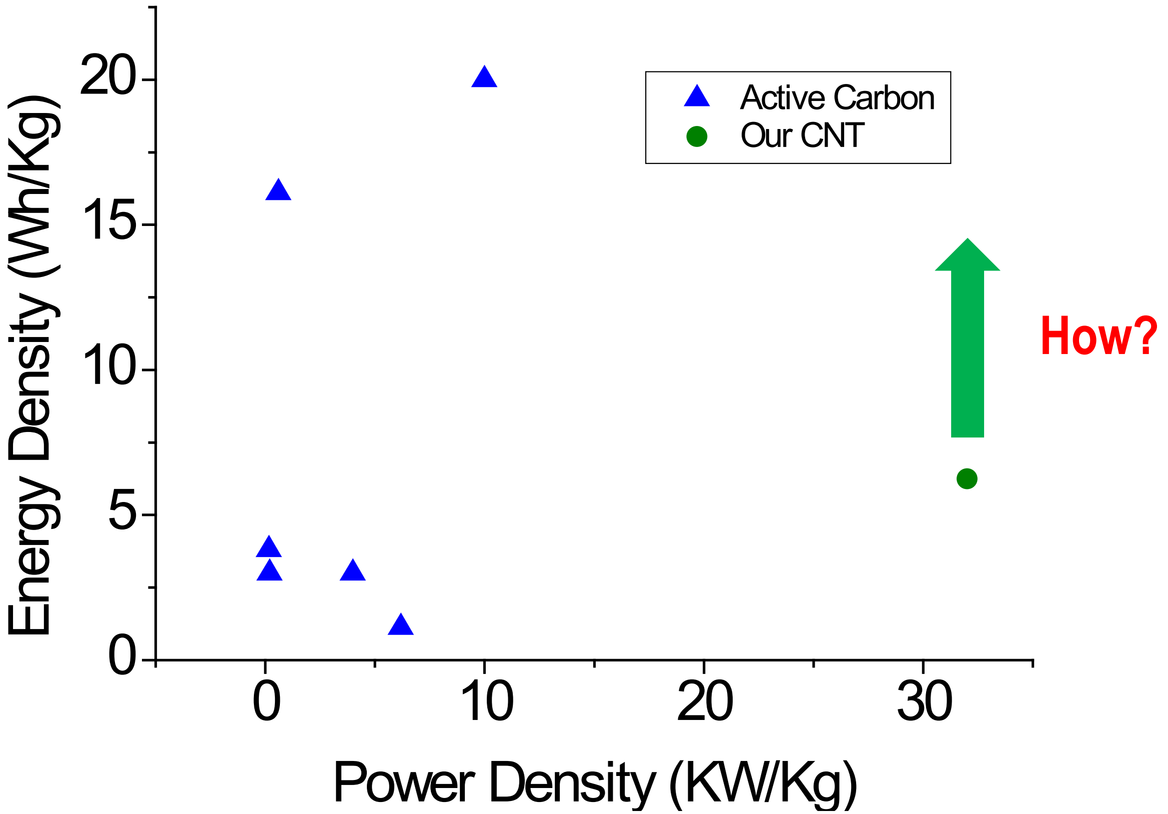

Refs: (All papers on electric double layer capacitor published in Journal of Power Sources in 2008&2009)
2009: K.-W. Nam et al.; W. Lu et al.; H. Guo et al.
2008: K. Kalinathan et al.; V. Khomenko et al.; J.A. Fernandez et al.

Functionalized CNT Forest Electrodes

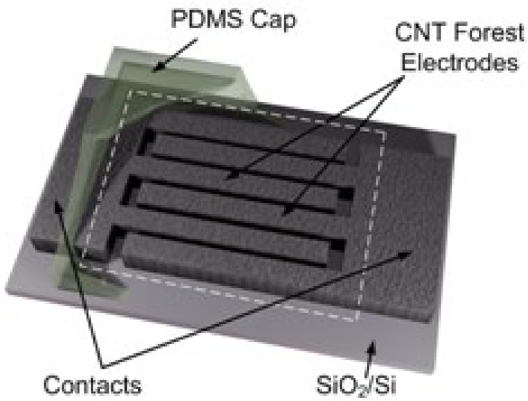

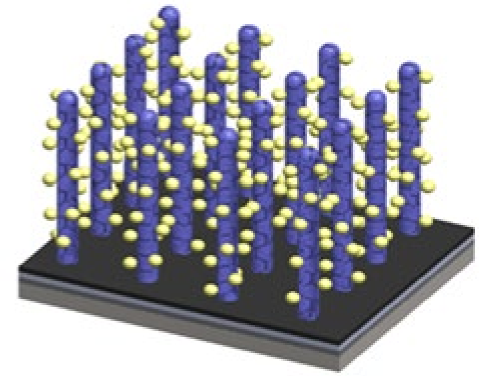

MEMS Supercapacitor

$$C_{SP} = \frac{C_I + C_E}{V} = \frac{\frac{\varepsilon}{d}A + C_E \uparrow}{V}$$

Principle of Pseudo-capacitor

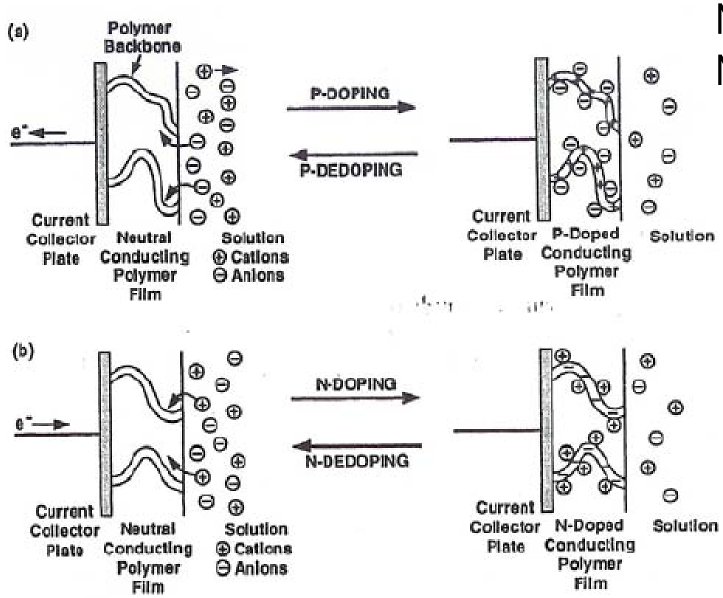

B. E. Conway. Electrochemical Supercapacitors, Scientific Fundamental and Technological Applications, Plenum Publishers, 1999.

Mechanism of pseudo supercapacitor

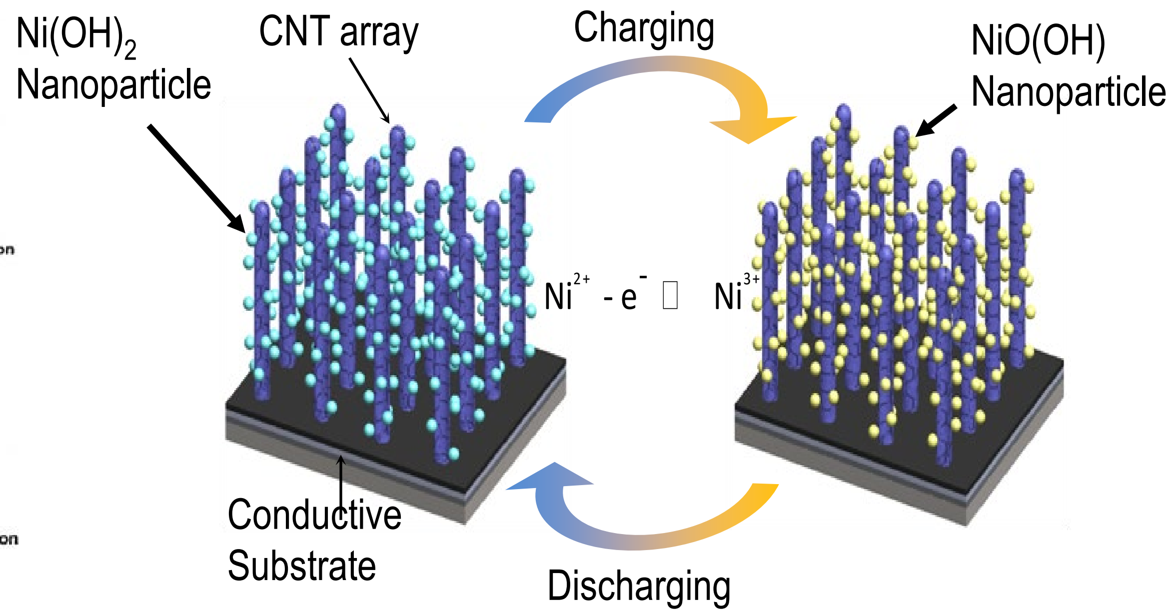

$$Ni(OH)_2 + OH^- \rightleftharpoons NiO(OH) + H_2O + e^-$$

- Pseudo supercapacitors balance between supercapacitor and battery
- Metal oxide (Mn, Ru, Ni, etc.) and conducting polymer all act as coating materials
- Electroplating is liquid phase, low cost and capable of selective deposition

Vacuum-enabled Infiltration

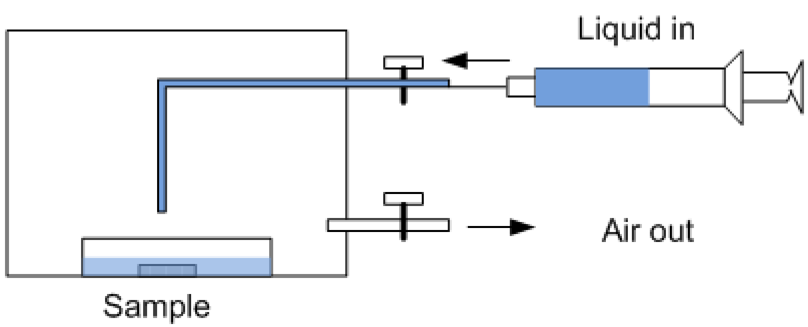

Basic procedures:

1. Load samples into the vacuum chamber
2. Hold on (>5min) in vacuum;
3. Fill in liquid until the sample is fully covered;
4. Hold on under liquid (>10min);
5. Vent and unload;
6. Continue with normal electroplating

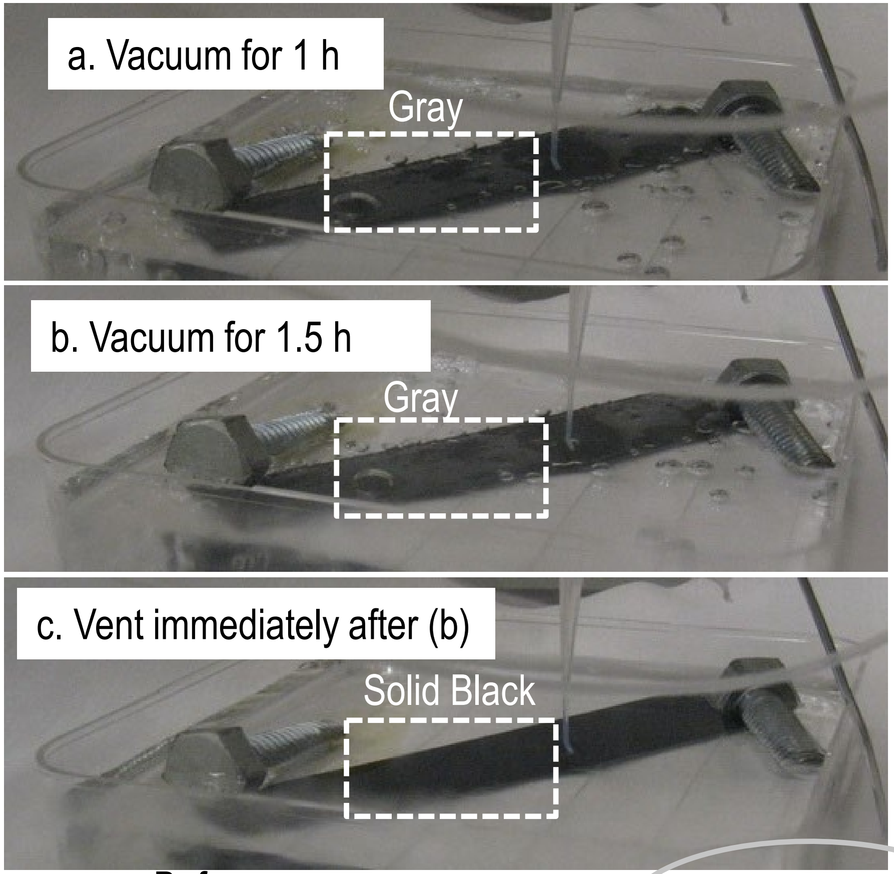

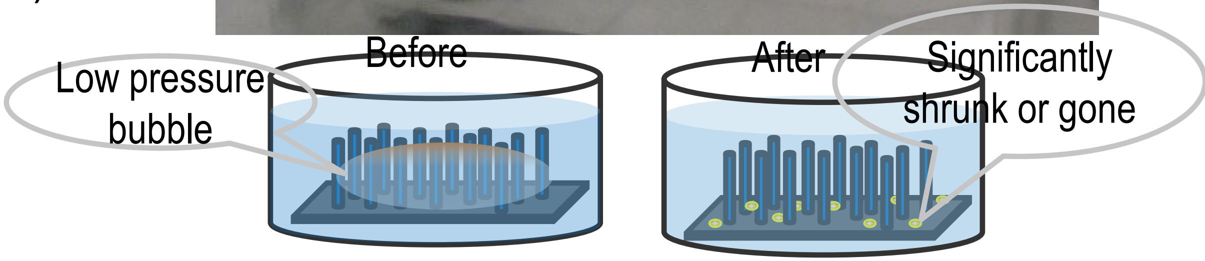

Electroplating results and analysis

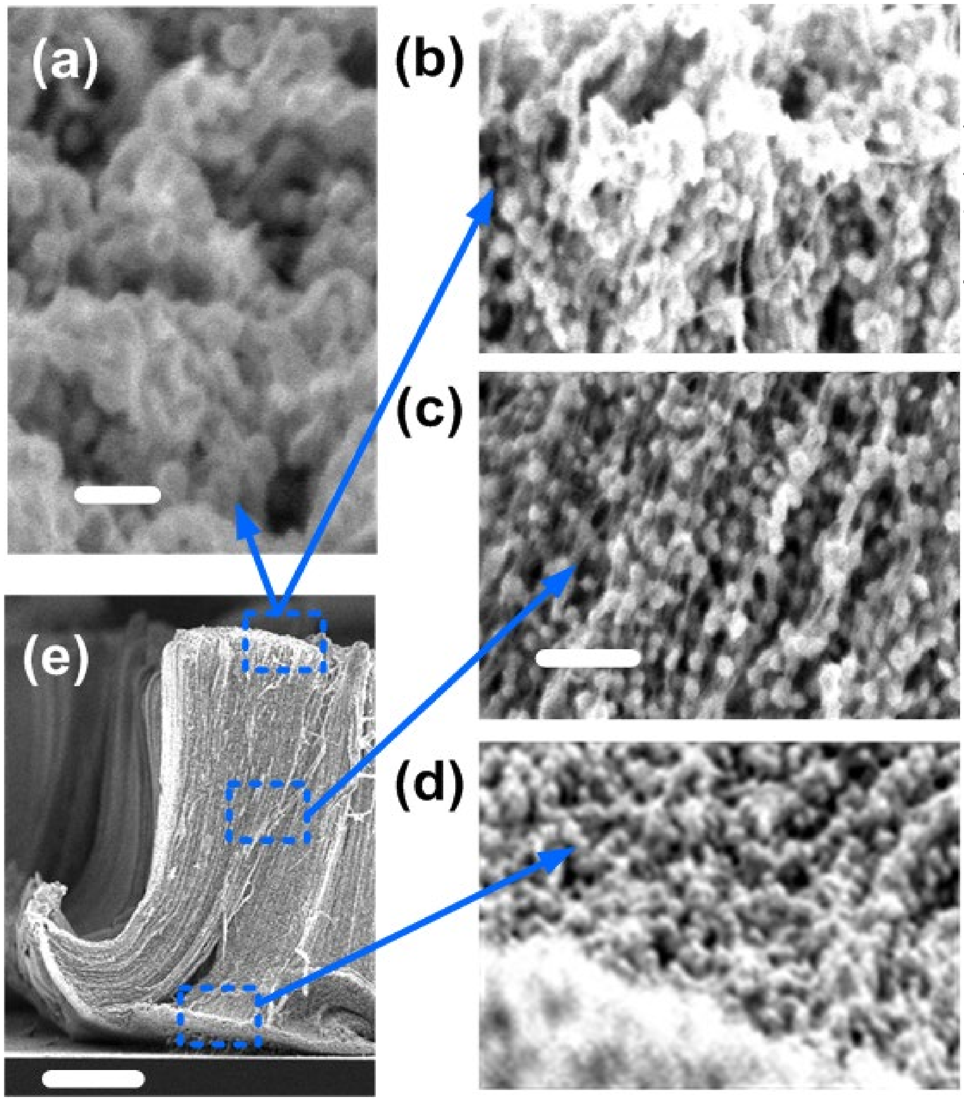

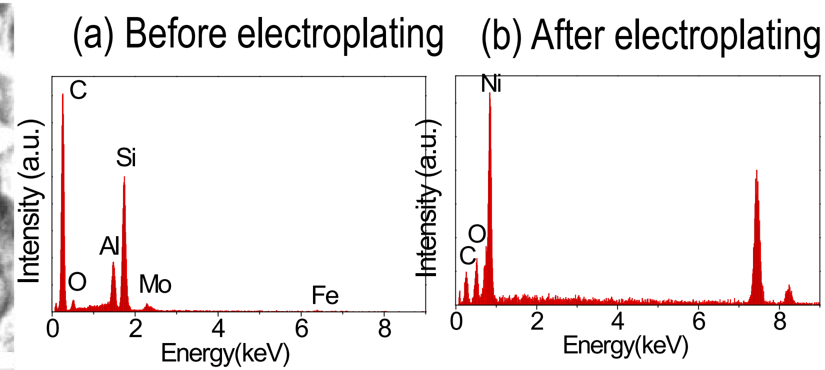

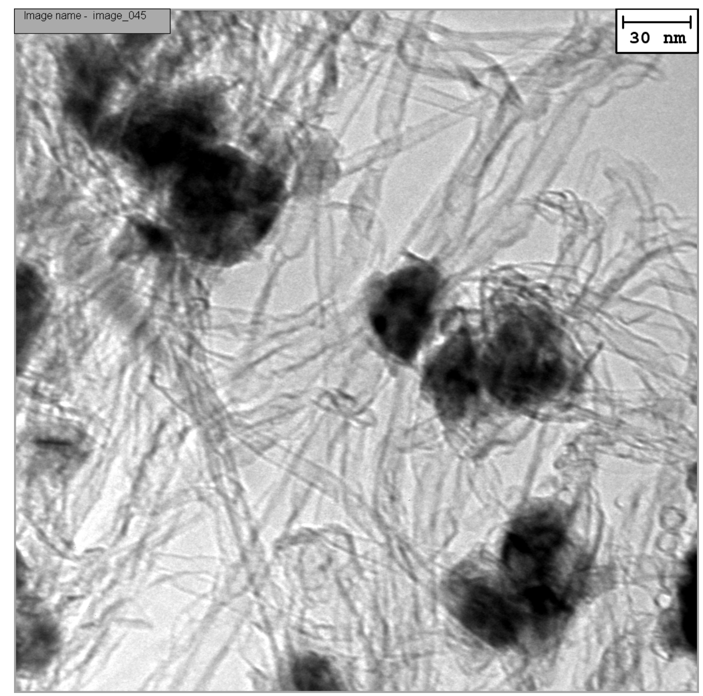

Performance of Ni-plated (G2) CNT supercapacitor

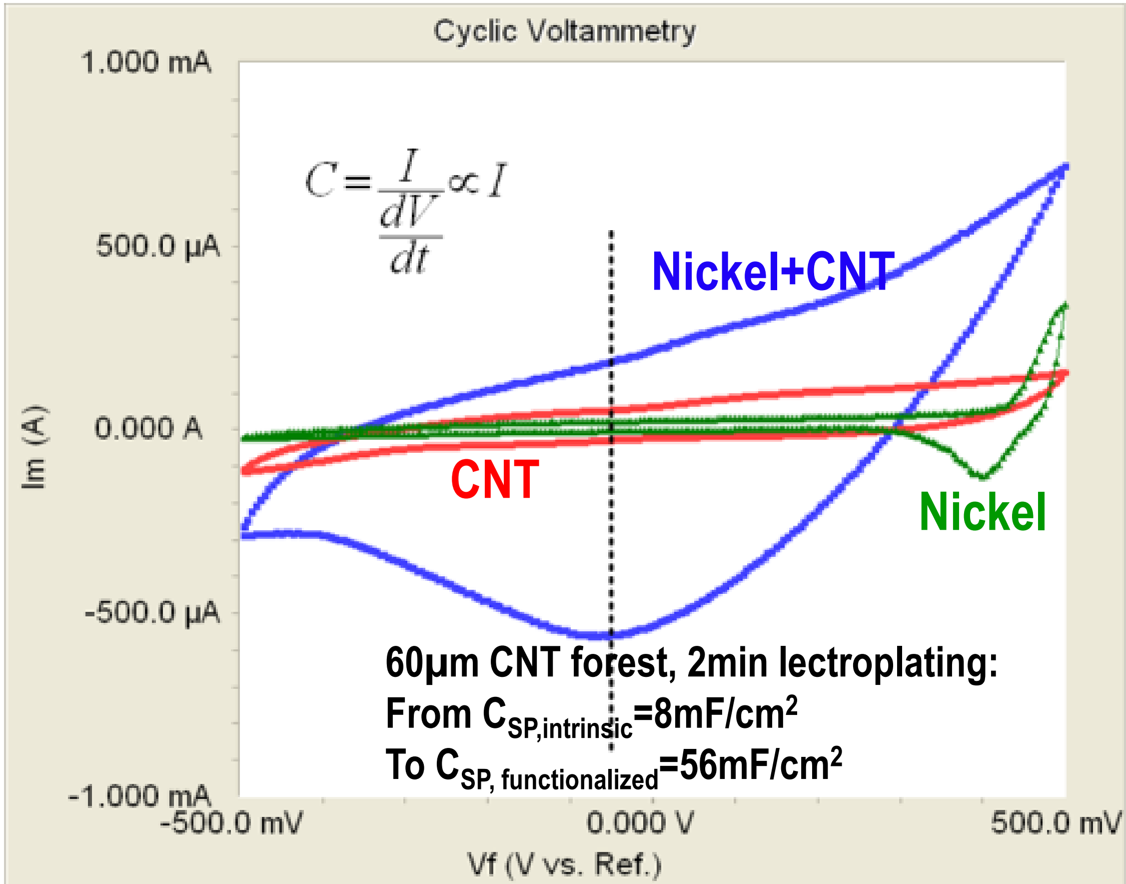

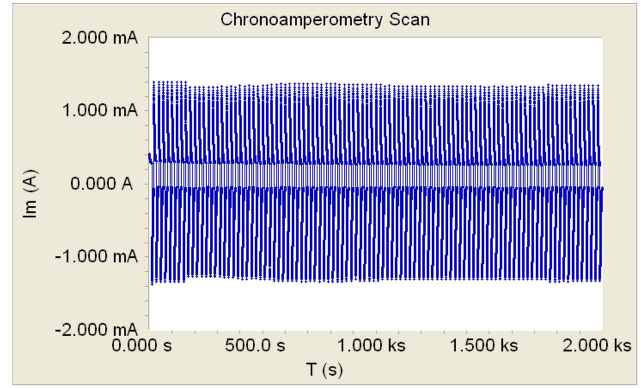

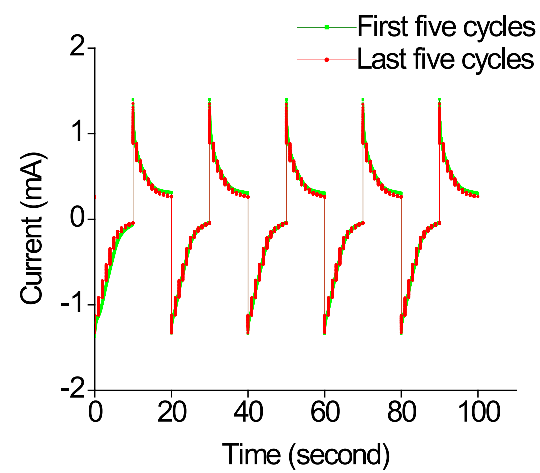

- Significantly enhance the energy density up to one order
- Robust operation of over100 times charge/discharge tests.

Ultra-Long CNTs

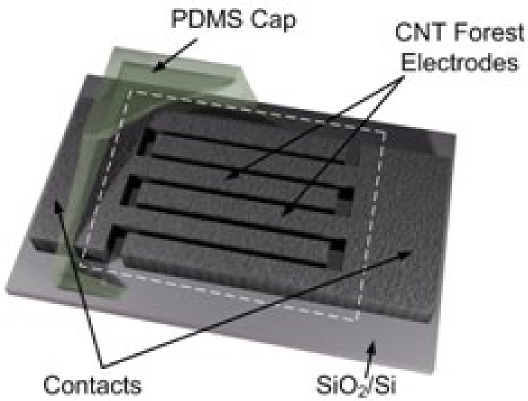

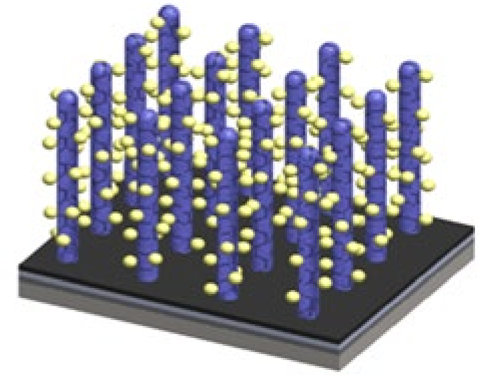

MEMS Supercapacitor

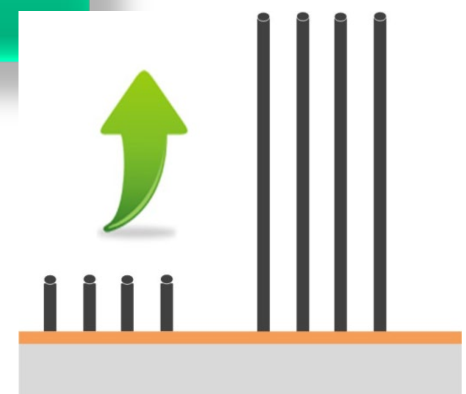

$$C_{SP} = \frac{C_I + C_E}{V} = \frac{\frac{\varepsilon}{d} A \uparrow + C_E}{V}$$

Exciting results of new CNT synthesis

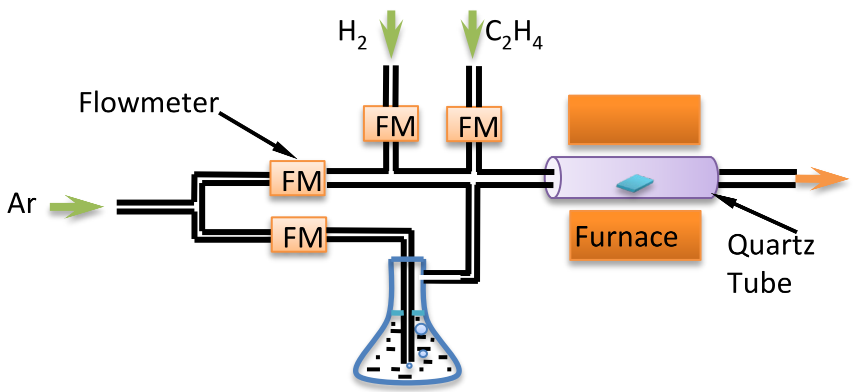

Water-assisted thermal CVD setup

Iijima, S, et al. Science, vol. 306, 2004,pp.1362

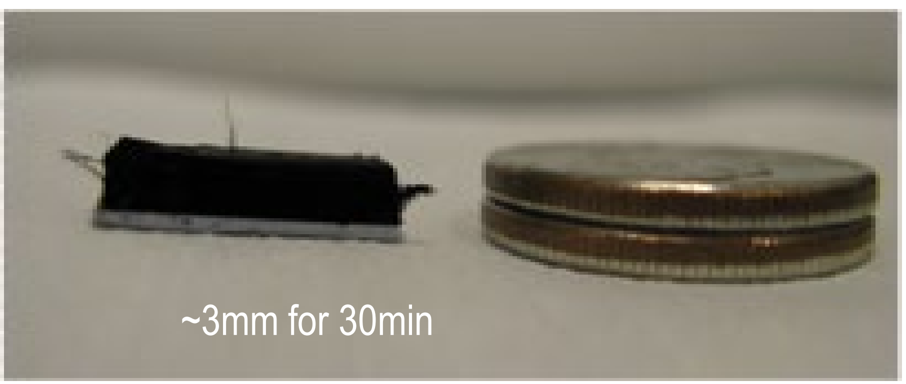

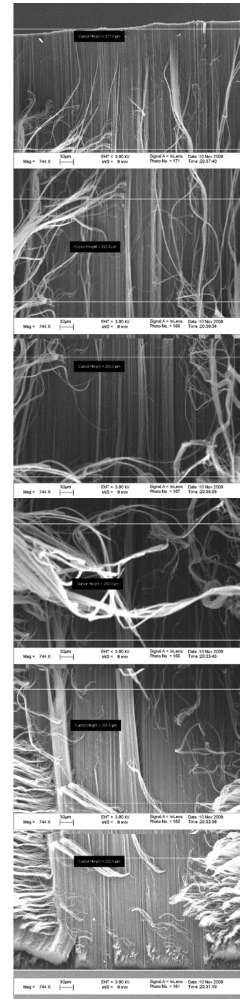

1542μm@5nm Fe, 30min

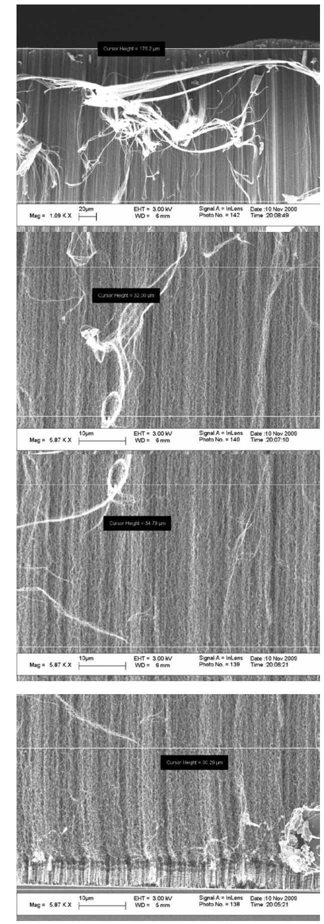

273μm@5nm Fe, 10min

Performance of ultra-long CNT supercapacitor

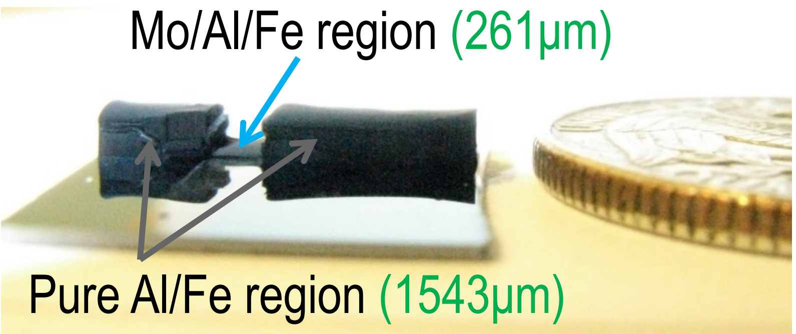

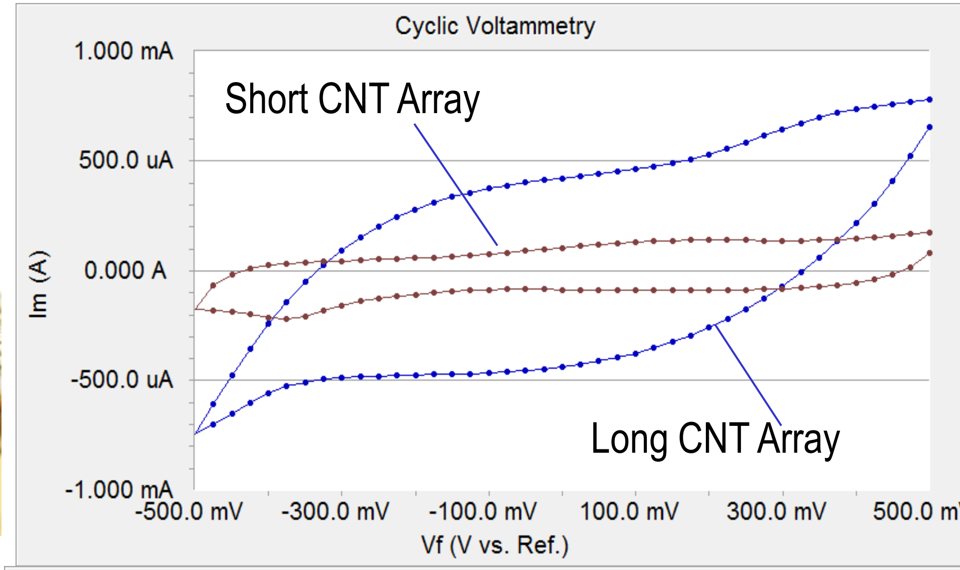

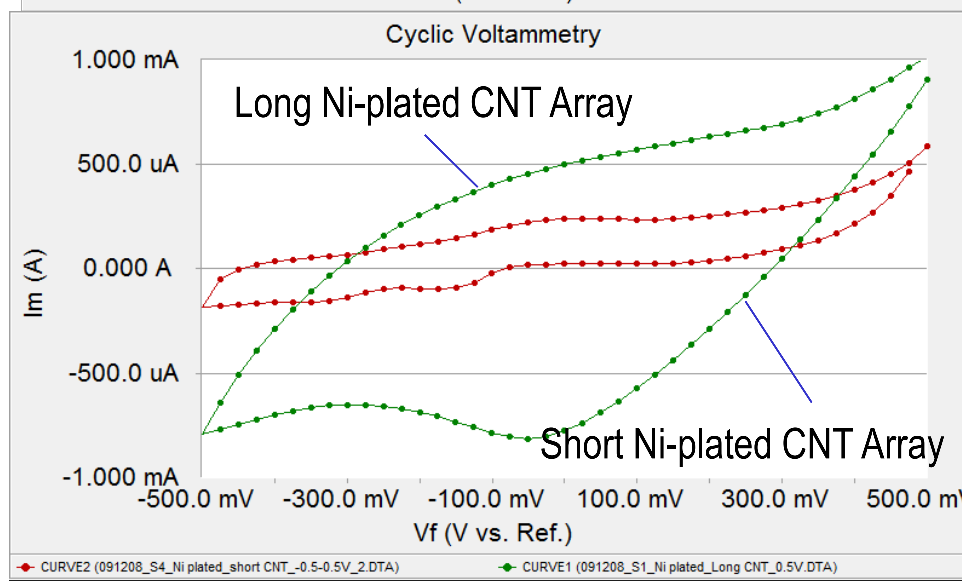

- Unsurprisingly, "wet growth" favors insulating substrate (No Mo)
- Performance in proportion to the height increase in both case
- Indirectly prove the uniform coating of nickel nanoparticles

Densified CNTs

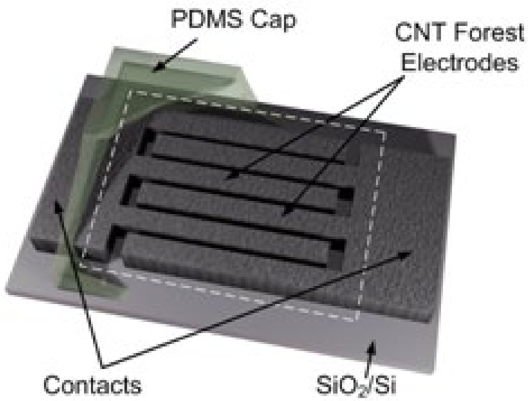

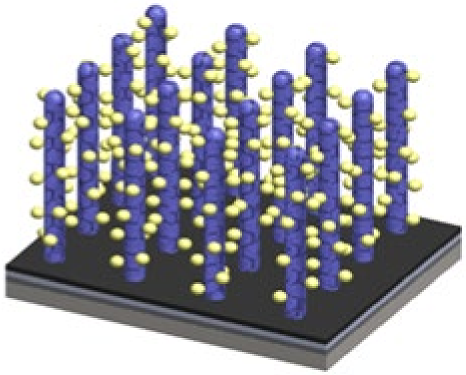

MEMS Supercapacitor

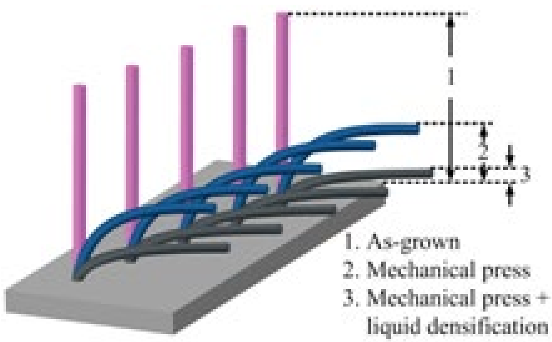

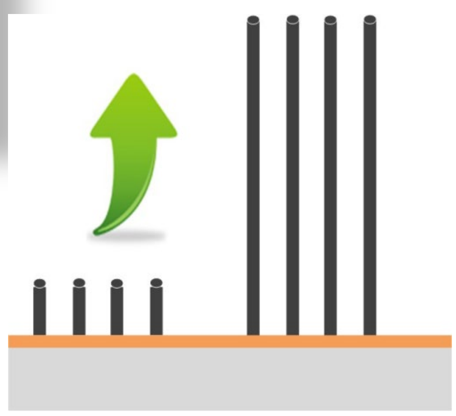

$$C_{SP} = \frac{C_I + C_E}{V} = \frac{\frac{\varepsilon}{d}A + C_E}{V \downarrow}$$

Liquid Densification

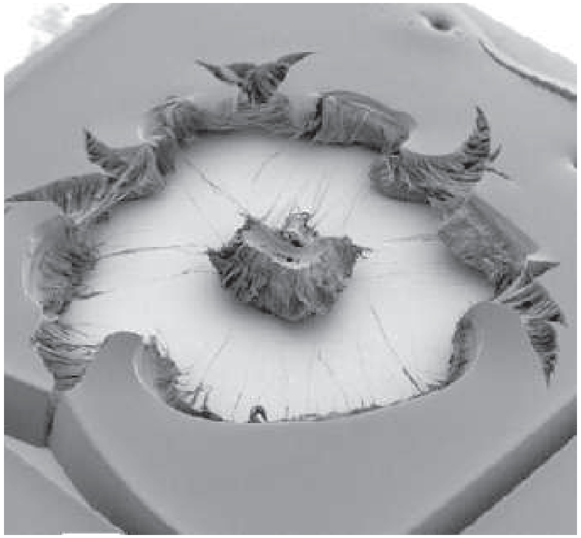

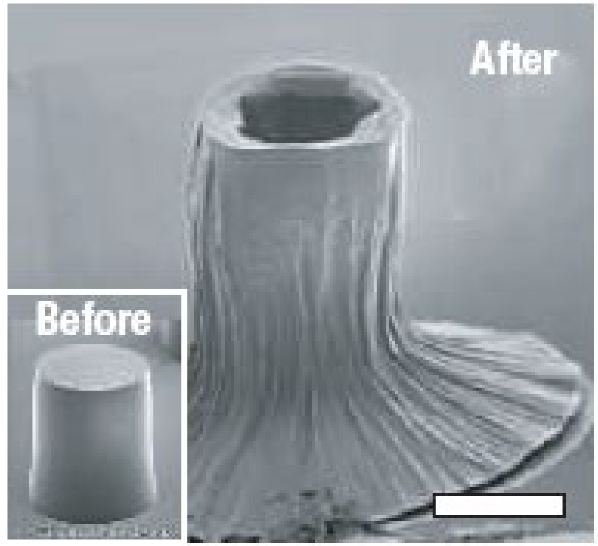

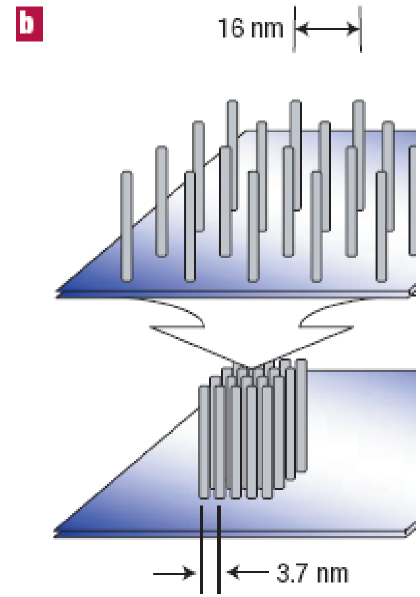

S. IIJIMA et al., nature materials, 5(2006)

- **Effects:** Astonishing volume collapse
- **Mechanism:** Zipping effects of Liquid (Surface tension based)
- **Structure:** High-densely packed and aligned
- **Material:** Retains the intrinsic properties (not harmed)
- **Challenge:** Can we control this process?

Pressing-guided collapse of CNT forests

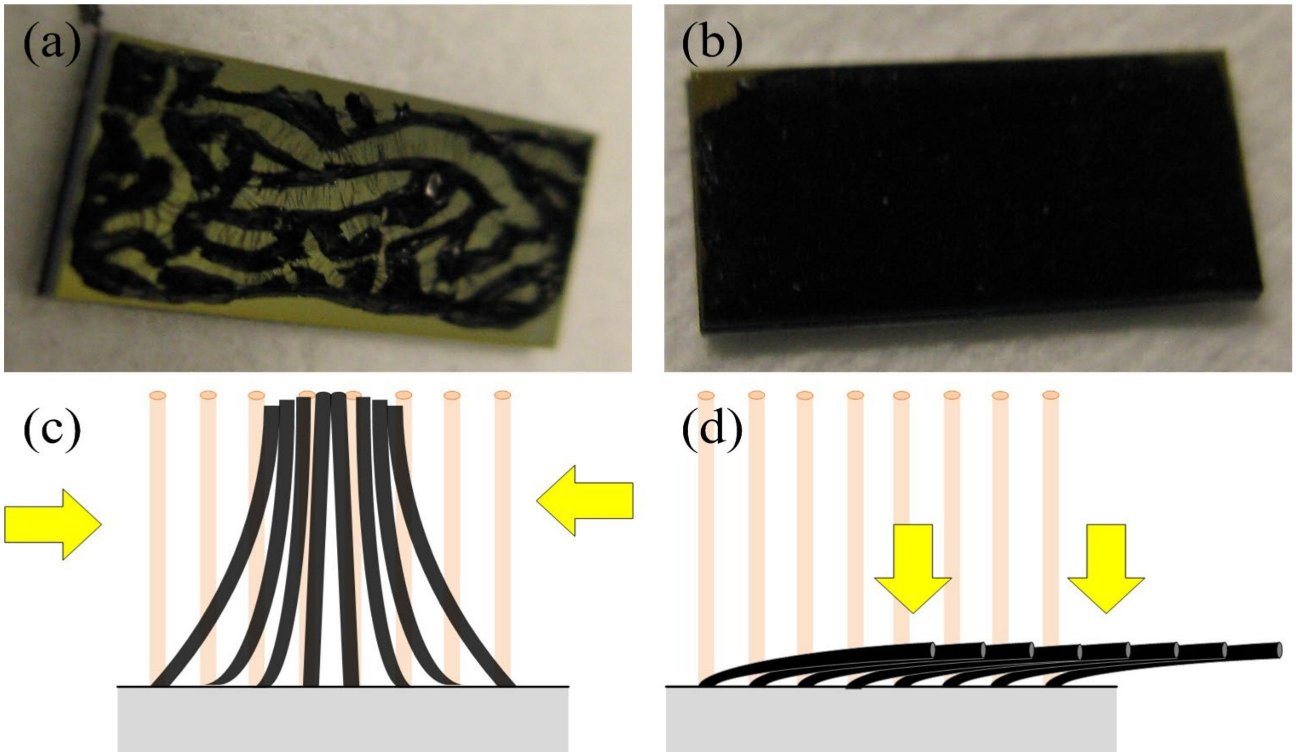

	Un-pressed	Pre-Pressed
Contraction	Lateral	Vertical
Controllable?	No, random	Yes, uniform

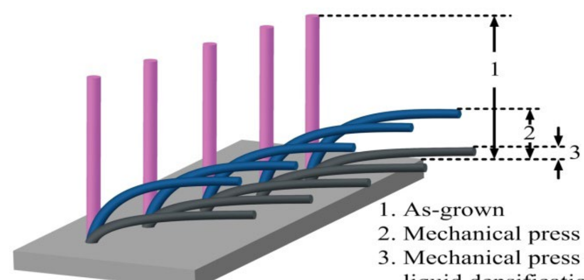

Highly-densely packed CNT forest

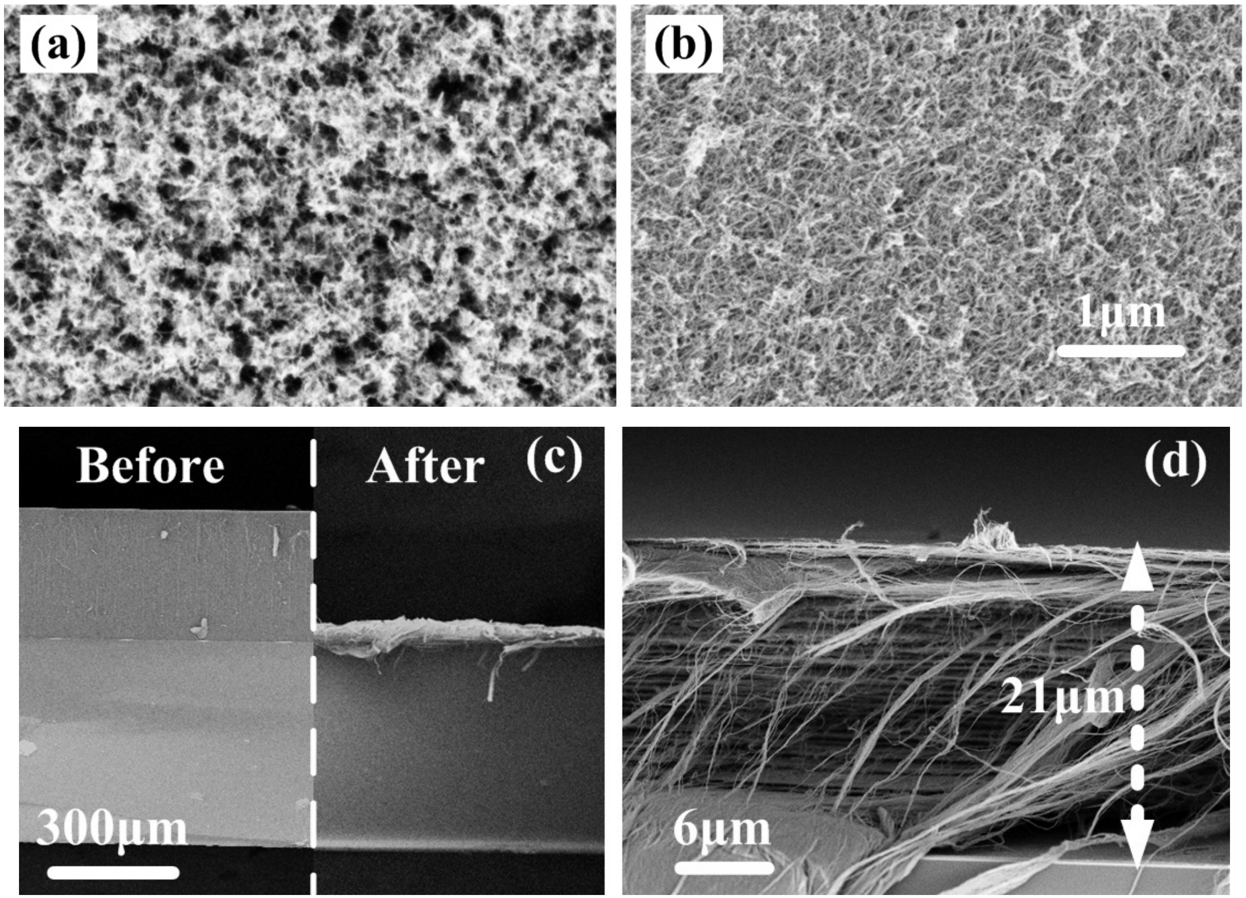

- Astonishing 16X times collapse
- Better smoothness
- Alignment retained

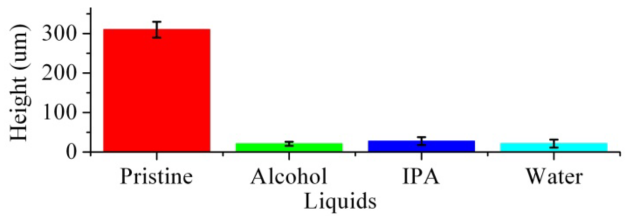

Supercapacitor using densely-packed CNT

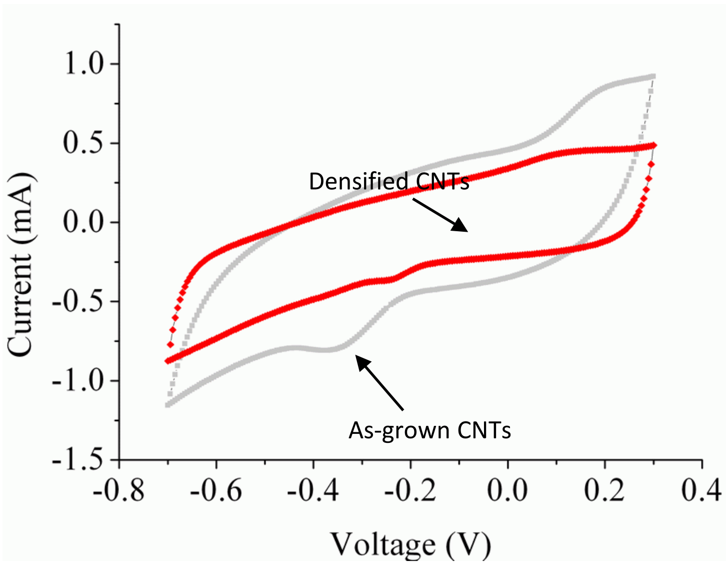

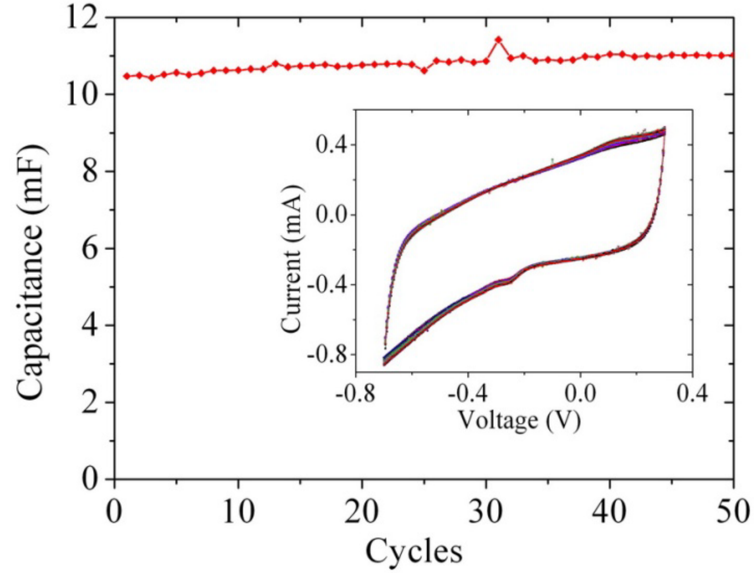

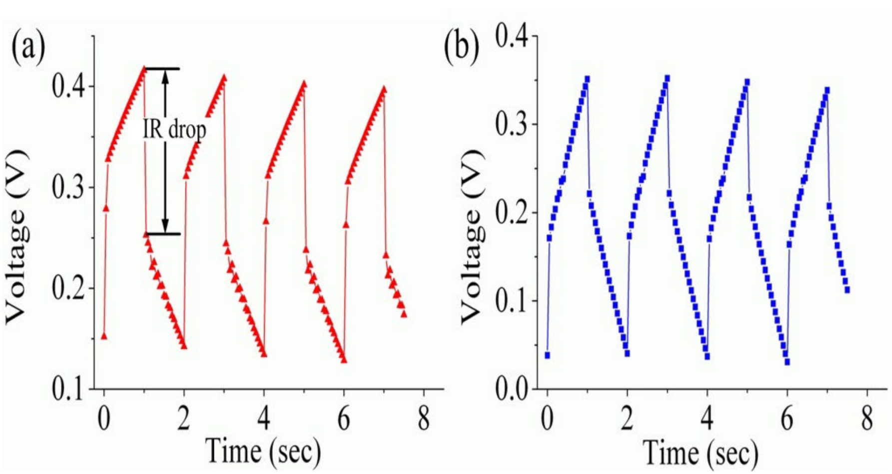

- CNT performance (surface area) is not compromised
- Gradually increasing performance due to better electrolyte penetration
- Decreased resistance due to numerous new “contacts”

Hybrid Supercapacitor/Battery

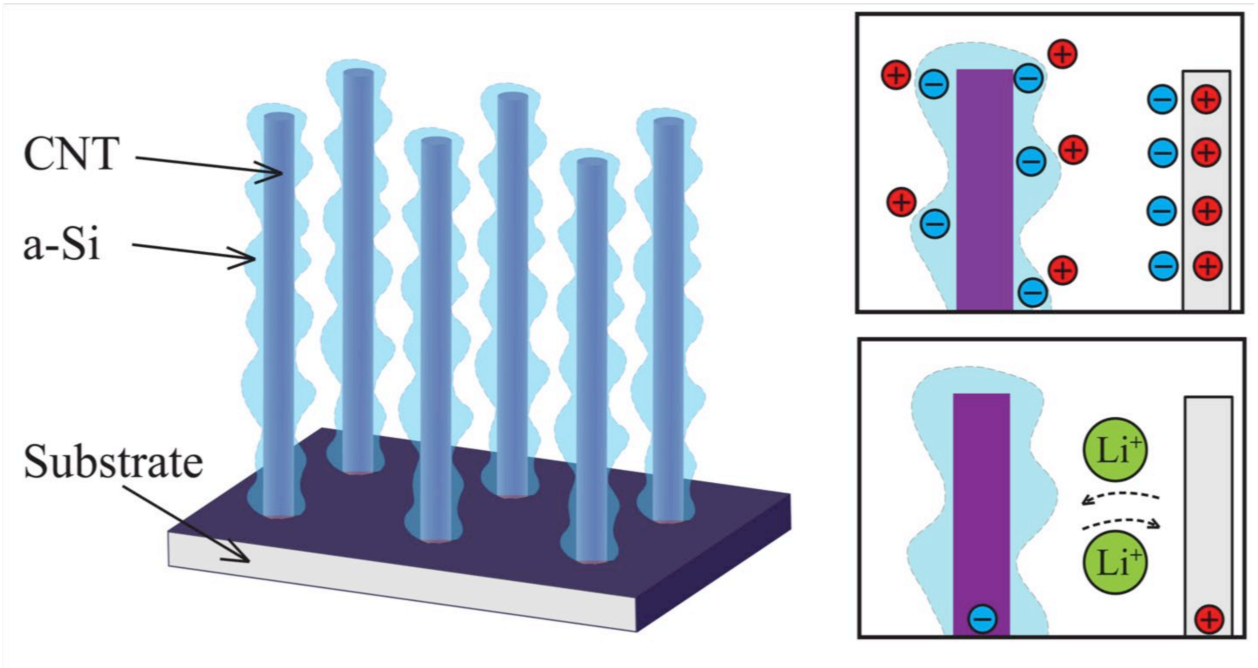

Silicon coating on vertically aligned carbon nanotubes:

- **Top inset:** usage in electrochemical double layer capacitors
- **Bottom inset:** usage in lithium ion batteries
- CNT forest shape is easily controlled by patterning the catalyst

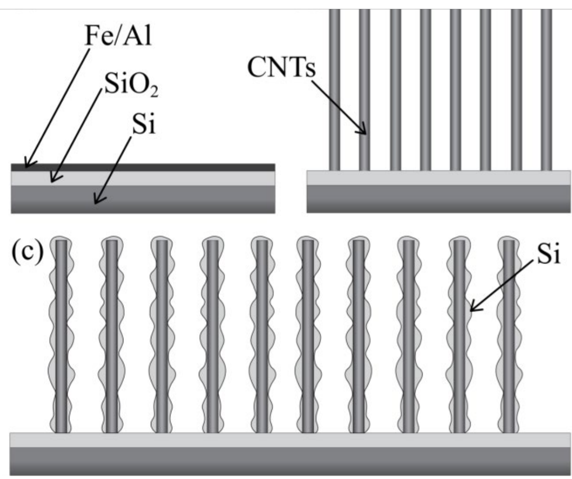

Main steps to fabricate CNT/Si-coated anode:

(a) Catalyst deposition

(b) CVD CNT growth

(c) Partial timed LPCVD silicon deposition

Silicon Coated CNT Forests

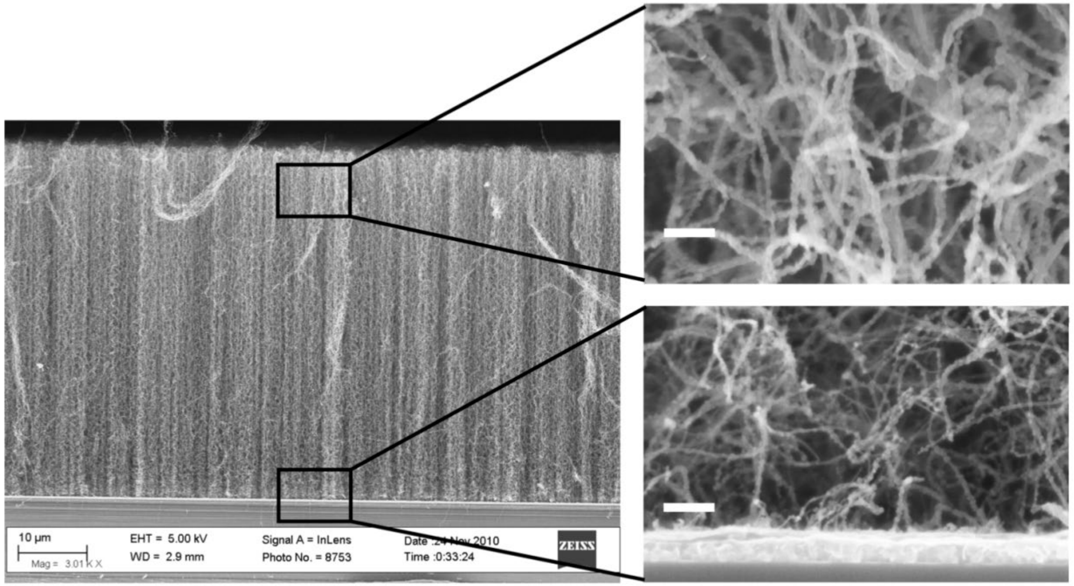

SEM images of cross section of Si-coated CNT forest:

- Top Inset: close view of Si deposition near top of forest
- Bottom inset: Close-up view of Si deposition at bottom of forest

Scale bars in insets are 200 nm

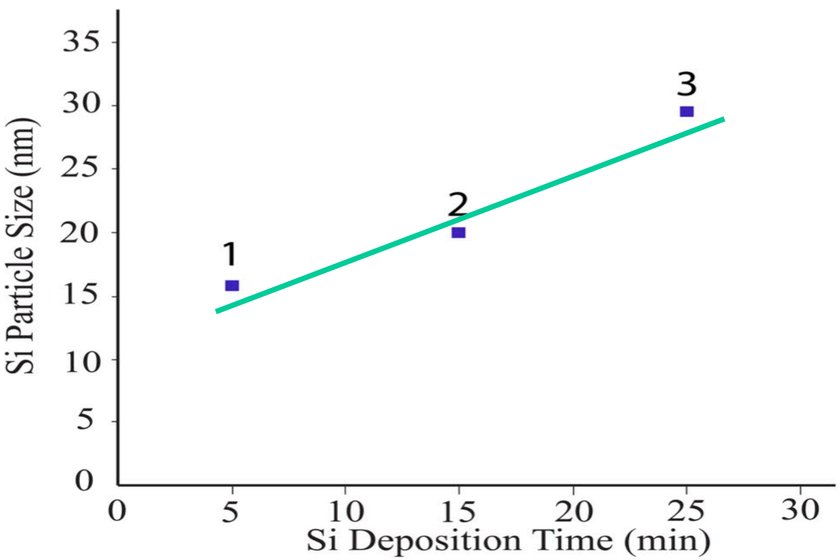

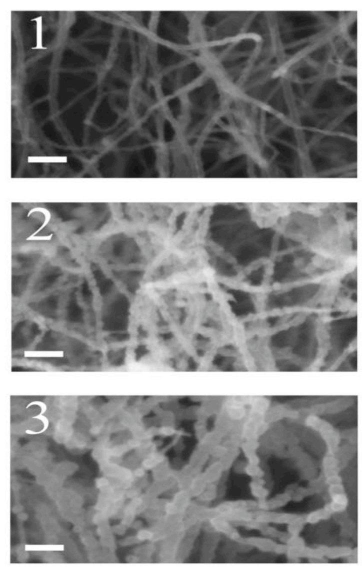

Si particle size over time of deposition and SEM image of forest after

1. 5 min Si deposition
2. 15 min Si deposition
3. 25 min Si deposition

Scale bars are 100 nm

Performance of Amorphous – Silicon Coated CNT Forests in a Supercapacitor Application

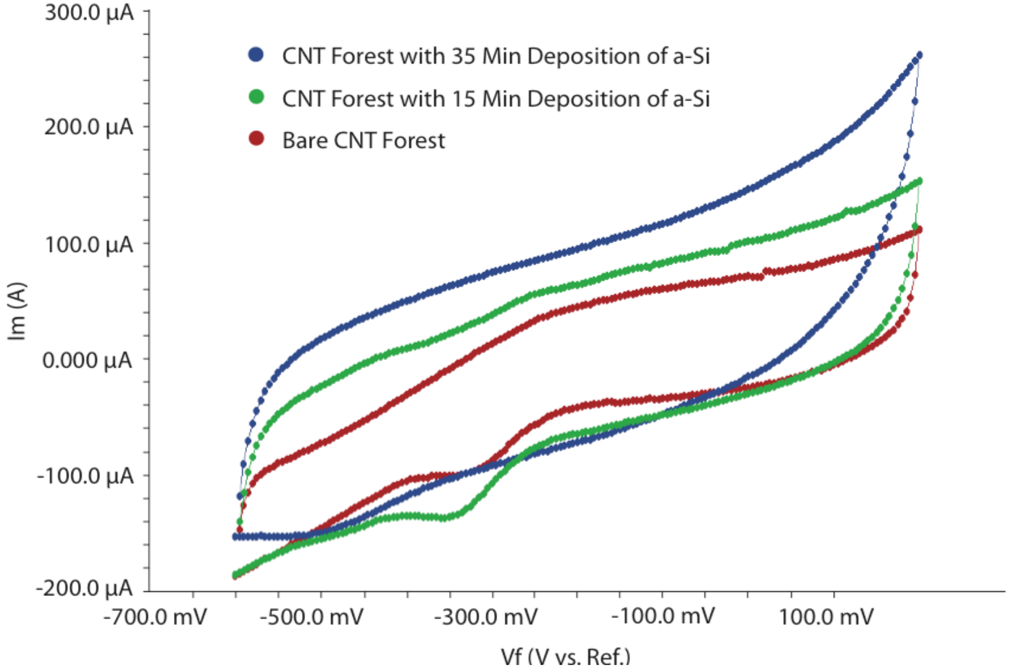

Measured cyclic voltammetry data of electrodes before (red) and after both 15 min (green) and 35 min (blue) a-Si deposition

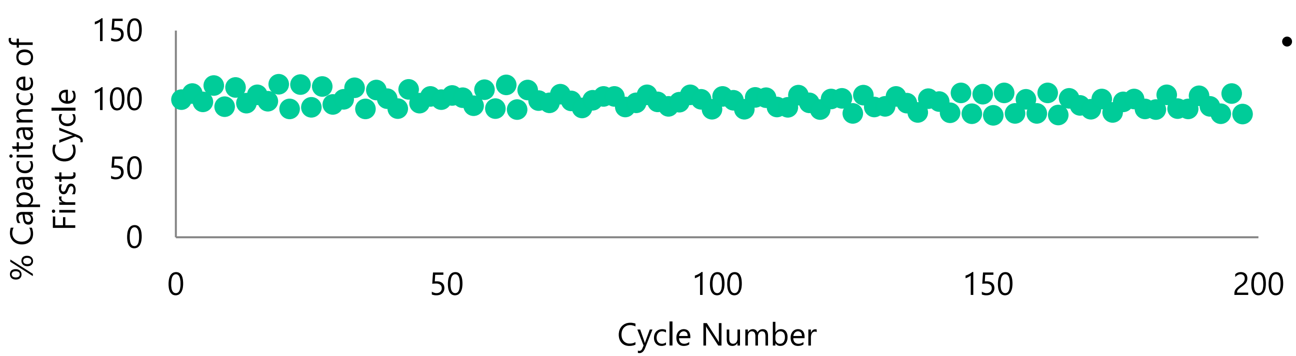

- Measured cycling performance of anode cycled from -0.6 to 0.2 V for 200 cycles
- The electrode is stable in capacitance (and hence energy density) over cycling

CVD + ALD

Integration of CNT & RuO_2

Journal of Materials Chemistry - A, Vol. 3, 15568-15575, 2015

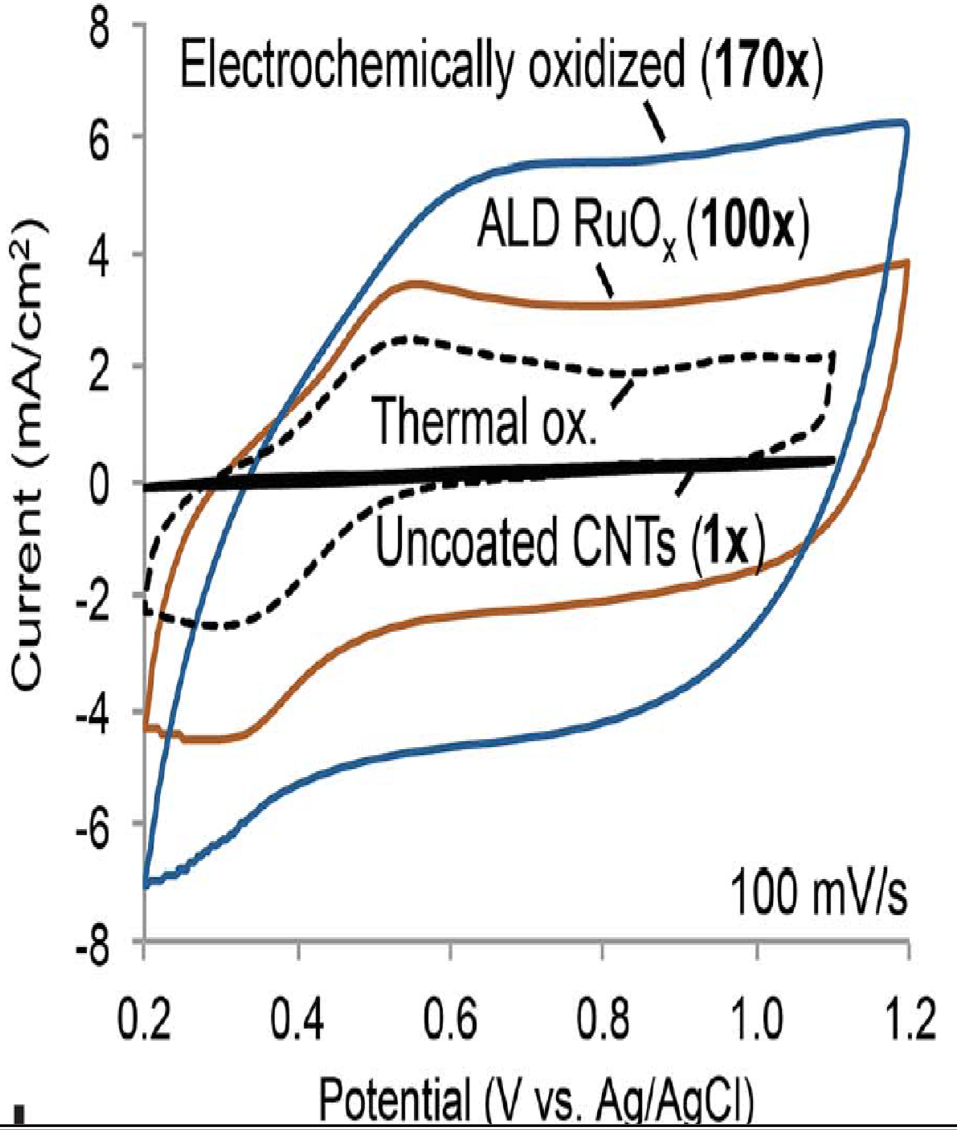

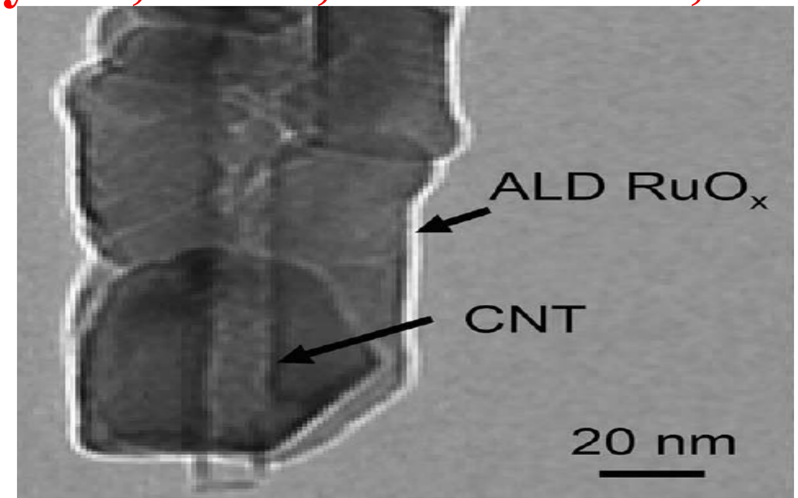

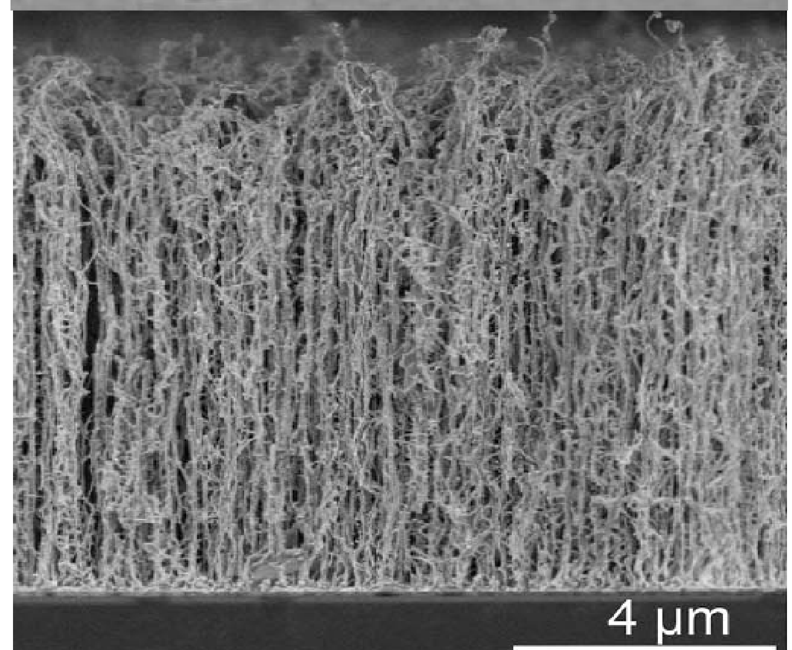

CVD + ALD

Integration of TiS_2 & CNT

Advanced Materials, Vol. 3, 15568-15575, 2015

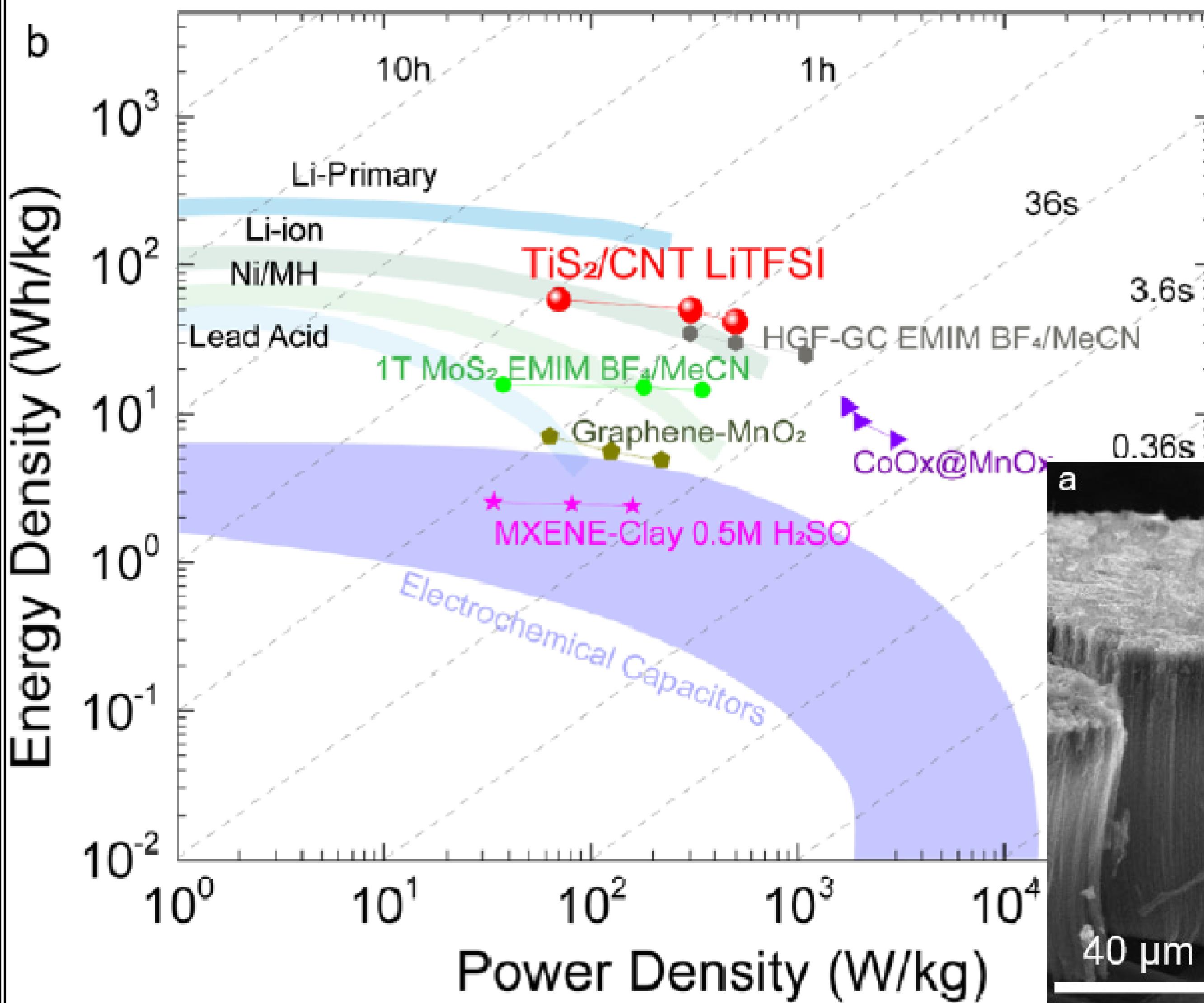

ACNT : High Capacitance
Long Cycling Lifetime

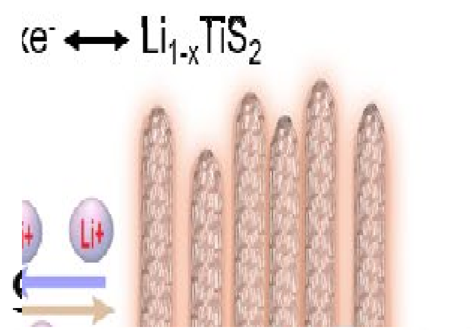

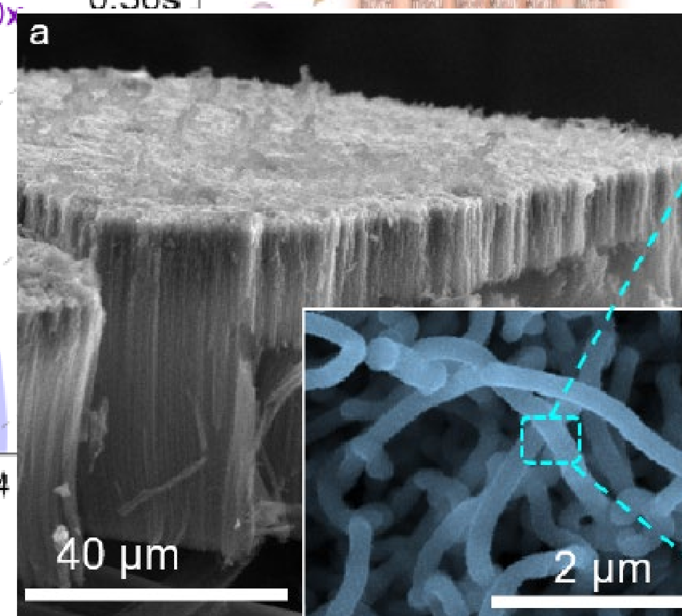

Summary

- Planar MEMS supercapacitors using CNT array electrodes have been demonstrated for the first time.
- Mo/Al/Fe metal stack layer has been innovatively proposed to make both high quality CNT and low-contact resistance.
- Vacuum-enabled electroplating has been proposed for pseudo CNT supercapacitor for 10x higher energy density
- Ultra-long CNT array has been synthesized using water-assisted CVD method for 3X higher energy density
- Pressing-guided densification has brought down the volume by 16X
- Four stages of supercapacitor, as-grown, Ni-electroplated (~10X), Ultra-long (~3X) and densification (~16X), have been successfully realized, with a total energy density enhancement of 480X
- Hybrid Supercapacitor/Battery is ongoing

Future Work

MEMS Hybrid Supercapacitor/Battery

- Doped polysilicon deposition in lieu of amorphous silicon for additional supercapacitor tests
  - Increase in defect sites leads to an increase in capacitance
- Lithium ion battery application